IMAGENET-OOD: DECIPHERING MODERN OUT-OF-DISTRIBUTION DETECTION ALGORITHMS

William Yang*, **Byron Zhang***, **Olga Russakovsky**
Department of Computer Science, Princeton University, Princeton, NJ, USA
{williamyang,zishuoz,olgarus}@cs.princeton.edu

ABSTRACT

The task of out-of-distribution (OOD) detection is notoriously ill-defined. Earlier works focused on new-class detection, aiming to identify label-altering data distribution shifts, also known as "semantic shift." However, recent works argue for a focus on failure detection, expanding the OOD evaluation framework to account for label-preserving data distribution shifts, also known as "covariate shift." Intriguingly, under this new framework, complex OOD detectors that were previously considered state-of-the-art now perform similarly to, or even worse than, the simple maximum softmax probability baseline. This raises the question: what are the latest OOD detectors actually detecting? Deciphering the behavior of OOD detection algorithms requires evaluation datasets that decouple semantic shift and covariate shift. To aid our investigations, we present ImageNet-OOD, a clean semantic shift dataset that minimizes the interference of covariate shift. Through comprehensive experiments, we show that OOD detectors are more sensitive to covariate shift than to semantic shift, and the benefits of recent OOD detection algorithms on semantic shift detection is minimal. Our dataset and analyses provide important insights for guiding the design of future OOD detectors.[1]

1 INTRODUCTION

Out-of-distribution (OOD) detection aims to identify test examples sampled from a different distribution than the training distribution. In the context of computer vision, an OOD detector is simply a post-hoc score calibration function that operates on a trained image classification model. Previous work has proposed tackling this problem from two perspectives: new-class detection and failure detection. In new-class detection, OOD detectors are expected to identify new object categories for the purpose of data collection and continual learning (Liu et al., 2020; Hendrycks et al., 2022; Wang et al., 2022; Liang et al., 2018; Kim et al., 2022). Recent works have motioned to shift the objective from new-class detection to the scenario of failure detection, where OOD detectors are expected to identify misclassified examples to promote the safety and reliability of deep learning models in real-world applications (Jaeger et al., 2023; Zhu et al., 2022; Averly & Chao, 2023; Guérin et al., 2023). However, evaluating OOD detectors via failure detection benchmarks yields one unanimous finding: no modern OOD detector surpasses the performance of the simple maximum softmax probability (MSP) (Hendrycks & Gimpel, 2017) baseline. In light of this drastic discrepancy, we need to take a step back to address the question: what are modern OOD detectors actually detecting?

Common literature in OOD detection separates distribution shifts into semantic (label-altering) and covariate (label-preserving) shifts (Hsu et al., 2020; Tian et al., 2021; Yang et al., 2021b). Understanding detection behavior for either type of shift requires proper evaluation datasets that decouple semantic shifts from covariate shifts (Yang et al., 2021a). Many OOD detection datasets (Wang et al., 2018; Hendrycks et al., 2021; Galil et al., 2023) set ImageNet-1K (Russakovsky et al., 2015) as in-distribution (ID) and subsets of ImageNet-21K (Deng et al., 2009) as out-of-distribution (OOD). Since ImageNet-1K is also a subset of ImageNet-21K, both datasets' class labels are derived from the WordNet (Fellbaum, 1998) hierarchy and the images share the same data collection process. However, these datasets often contain contamination from ID images, which violates one of the key

*Equal contribution.
[1] Code and data is at https://github.com/princetonvisualai/imagenetood

assumptions of OOD detection for both new-class and failure detection (Bitterwolf et al., 2023). Consequently, several human-annotated datasets have been constructed, though using data sources outside the ImageNet family (Hendrycks et al., 2022; Wang et al., 2022; Bitterwolf et al., 2023), introducing unforeseen covariate shifts due to changes in the data source and collection process.

In this paper, we design an OOD detection dataset that can accurately assess the impact of semantic shift without the influence of covariate shifts. Concretely, we introduce **ImageNet-OOD**, a clean, manually-curated, and diverse dataset containing 31,807 images from 637 classes for assessing semantic shift detection using ImageNet-1K as the ID dataset. ImageNet-OOD minimizes covariate shifts by curating images directly from ImageNet-21K while removing ID contamination from ImageNet-1K through human verification. We identify and remove multiple sources of semantic ambiguity arising from inaccurate hierarchical relations in ImageNet labels. Additionally, we remove images with visual ambiguities arising from the inconsistent data curation process of ImageNet. Using ImageNet-OOD and three ImageNet-1K-based covariate shift datasets, we perform extensive experiments on nine OOD detection algorithms across 13 network architectures, from both new-class detection and failure detection perspectives to make the following findings:

1. Modern OOD detection algorithms are even *more* susceptible towards detecting covariate shifts than semantic shift compared to the baseline MSP (Hendrycks & Gimpel, 2017).
2. In ImageNet-OOD, which exhibits only semantic and limited covariate shift, modern OOD detection algorithms yield very little improvement over the baseline on new-class detection.
3. Modern OOD detection algorithms only improve on previous benchmarks by ignoring incorrect ID examples rather than detecting OOD examples, causing performance disparity between the task of new-class detection and failure detection.

2 EXISTING DEFINITIONS AND FORMULATIONS

Problem Setup. For image classification, a dataset $D_{tr} = \{(x_i, y_i); x_i \in \mathcal{X}, y_i \in \mathcal{Y}\}$ sampled from training distribution $P_{tr}(x, y)$ is used to train some classifier $C : \mathcal{X} \to \mathcal{Y}$. In real-world deployments, distribution shift occurs when classifier C receives data from test distribution $P_{te}(x, y)$ where $P_{tr}(x, y) \neq P_{te}(x, y)$ (Moreno-Torres et al., 2012). An OOD detector is a scoring function s that maps an image x to a real number $\mathbb{R}$ such that some threshold τ arrives at a detection rule f:

$$f(x) = \begin{cases} \text{in-distribution} & \text{if } s(x) \geq \tau \\ \text{out-of-distribution} & \text{if } s(x) < \tau \end{cases} \tag{1}$$

Common changes within the data distribution fall under two categories: covariate shift, which is label-preserving (i.e. concerns examples only from training classes), and semantic shift, which is label-altering (concerns examples only from new classes).

Covariate Shift. Covariate shift occurs in the test data when the marginal distribution with respect to the image differs from the training data: $P_{tr}(x) \neq P_{te}(x)$ (Yang et al., 2021b), while the label distribution remains fixed: $P_{tr}(y|x) = P_{te}(y|x)$. In this work, we will use three popular datasets with covariate shifts with respect to ImageNet-1K (Russakovsky et al., 2015): ImageNet-C (Hendrycks & Dietterich, 2019), ImageNet-R (Hendrycks et al., 2020), and ImageNet-Sketch (Wang et al., 2019).

Semantic Shift. Semantic shift occurs when a given set of semantic labels $Y_{tr} \subset \mathcal{Y}$ from the training distribution and semantic labels $Y_{te} \subset \mathcal{Y}$ from a test distribution have the following property: $Y_{tr} \cap Y_{te} = \emptyset$, such that $P_{tr}(y) = 0 \; \forall y \in Y_{te}$. To best study the effect of semantic shifts, we propose a new dataset, ImageNet-OOD, that minimizes the degree of covariate shifts.

Evaluation. Many OOD detection benchmark commonly use AUROC as a threshold free way of estimating detection performance by calculating the area under false positive rate vs. true positive rate curve, considering ID as positive and OOD as negative.

Classical Approach: New-class Detection. The majority of work in OOD detection has formulated the problem as new class-detection: the notion of ID is defined by the class labels of the data

source and therefore is model agnostic. In other words, an image x is considered ID if it comes from a class $y \in Y_{tr}$ and OOD otherwise. OOD detection with this goal focuses exclusively on semantic shift: the detection of novel classes. Although the objective is analogous to that of Open-Set Recognition (Vaze et al., 2022), previous OOD detection works often motivated this goal to prevent model failures (Yang et al., 2021b). We provide more intricate discussion on the subtle differences in task formulation of previous OOD detection works in Section A of the Appendix.

Modern Approach: Failure Detection. Recent works argued to approach the OOD detection problem from the first principle. Instead of defining "ID" and "OOD" with regard to the data sources, the distinction is directly specified by the model's prediction. An image is ID if the model correctly classifies an image and OOD otherwise. These recent works converged on the conclusion that recent advances in OOD detection do not result in any improvement for the task of failure detection (Jaeger et al., 2023; Guérin et al., 2023; Zhu et al., 2022; Averly & Chao, 2023).

3 IMAGENET-OOD: A CLEAN SEMANTIC OOD DATASET

Recent works in OOD detection have primarily focused on failure detection, but new-class detection is still relevant in practice with the growing interest in adaptive learning systems (Kim et al., 2022; He & Zhu, 2022). Consequently, accurate assessment of OOD detection algorithms on semantic shift is very important and needs to be disentangled from covariate shift. Unfortunately, previous datasets were not carefully constructed, leading to contamination from ID classes and unintended covariate shifts. We highlight the shortcomings of past OOD datasets and introduce ImageNet-OOD, a carefully curated, semantic OOD dataset designed to overcome these challenges.

3.1 PITFALLS OF EXISTING SEMANTIC SHIFT DATASETS

Early evaluation frameworks in OOD detection primarily use small datasets such as CIFAR-10, CIFAR-100 (Krizhevsky, 2009), SVHN (Netzer et al., 2011), and MNIST (Deng, 2012), but their low-resolution and limited number of classes fail to extend to real-world conditions. Consequently, the outcomes of OOD detection methods in these restricted environments can substantially deviate from those in expansive settings. To include more diverse scenarios, recent OOD detection datasets often designate ImageNet-1K as the ID dataset (Hendrycks et al., 2022; Huang & Li, 2021; Galil et al., 2023). Nevertheless, these contemporary datasets frequently present issues, such as semantic or visual ambiguities and introduction of unnecessary covariate shifts.

Semantic Ambiguity. Several existing datasets overlook the hierarchical relations in ImageNet labels, leading to ambiguity in deciding whether a semantic concept is OOD. For example, ImageNet-O (Hendrycks et al., 2021) contains images from the class "pastry dough," which is contained in the "dough" class in ImageNet-1K. We also observe this contamination in OOD datasets that do not utilize ImageNet-21K classes, such as Species (Hendrycks et al., 2022). For example, the ImageNet-1K dataset contains the class "Agaric", which includes the Species class "Agaric Xanthodermus."

Visual Ambiguity. Although several datasets remove ID contamination through human filtering, they overlook visual ambiguity attributed to the intricacies in the data collection process of ImageNet. OOD classes can show up in ID images even though the ID and OOD classes are far away on the WordNet semantic tree (Fellbaum, 1998). For example, the C-OOD benchmark (Galil et al., 2023) contains the class "basin," while ImageNet-1K contains the class "lakeside." While "basin" is technically OOD, many images from the "lakeside" and "basin" classes are visually indistinguishable, and thus, can be labeled interchangeably.

Unnecessary Covariate Shifts. Several common OOD datasets used when ImageNet-1K is designated as ID include iNaturalist (Horn et al., 2018), SUN (Xiao et al., 2010), and Texture (Cimpoi et al., 2014). However, these datasets come from very specific domains and thus lack the semantic diversity that is reflected in real-world scenarios. Recent works such as NINCO (Bitterwolf et al., 2023) and OpenImage-O (Wang et al., 2022) encourage semantic diversity through manual selection of OOD images. However, due to the limited number of images, limited number of OOD classes, and/or deviation from the original ImageNet data collection procedure, the resulting dataset can potentially introduce hidden covariate shifts that OOD detection algorithms can exploit.

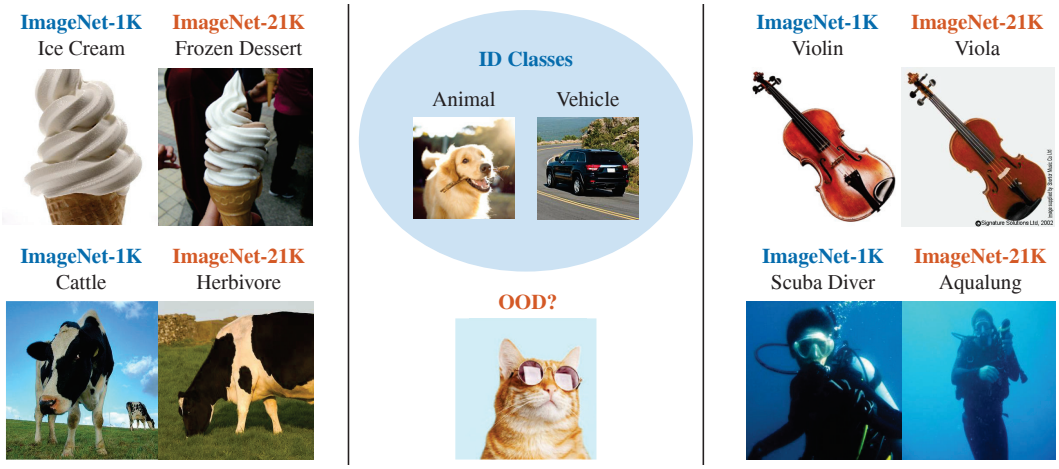

Figure 1: **Removing ambiguities in ImageNet-OOD.** We identify classes in ImageNet-21K which should *not* be included in the ImageNet-OOD dataset, since it would be ambiguous whether they are truly OOD with respect to the ImageNet-1K classes. *Left: Semantic Ambiguity.* "Frozen Dessert" in ImageNet-21K (Hendrycks et al., 2021) should not be considered OOD as it is a hyponym of "Ice Cream." Additionally, classes associated with organism is problematic in the WordNet hierarchy: "Herbivore" contains images from the ImageNet-1K class "Cattle" but it is neither a hypernym or a hyponym. *Middle: Semantically-grounded Covariate Shifts.* A dog vs. vehicle classifier can also be thought of as an animal vs. vehicle classifier. Given this classifier, it is unclear whether "cat" should be considered OOD. *Right: Visual Ambiguity.* "Violin" and "Viola" or "Scuba Diver" and "Aqualung" are visually indistinguishable to human labelers, leading to potential annotation error.

3.2 Construction of ImageNet-OOD

We start with the 1000 ImageNet-1K classes as ID. These classes are directly sampled from ImageNet-21K, which contains images illustrating the 21K nodes in the WordNet semantic tree (Fellbaum, 1998). We begin the construction of ImageNet-OOD with a pool of candidate classes from the processed version of ImageNet-21K (Ridnik et al., 2021). To reduce semantic ambiguity, we iteratively remove classes based on the following criteria:

All ImageNet-1K Classes, Their Hypernyms, and Hyponyms. Classes in ImageNet-1K are simply a subset of classes in ImageNet-21K according to the WordNet semantic tree. Since ImageNet-21K and ImageNet-1K followed the same data collection procedure, the degree of unwanted covariate shift is minimized (Galil et al., 2023). Consequently, these datasets often propose selecting OOD images from the set of ImageNet-21K classes that are disjoint from ImageNet-1K classes (Wang et al., 2018; Hendrycks et al., 2021). However, the hierarchical structure of WordNet allows hypernyms (semantic ancestors) and hyponyms (semantic descendants) of ImageNet-1K classes to contain ID images (*e.g.* "Ice Cream" vs. "Frozen Dessert" in Fig. 1 *Left*). We remove hypernyms and hyponyms of ID classes to promote accurate reflection of OOD detection performance.

Hyponyms of "Organism". Natural beings in WordNet and ImageNet-21K are categorized by both technical biological levels and non-technical categories, which leads to inconsistencies in hierarchical relations. For instance, although "Herbivore" is intuitively a hypernym of the ID class "Cattle," such a relationship is not captured by the WordNet semantic tree. Therefore, we avoid this type of ambiguity by removing all the hyponyms of "Organism."

Semantically-grounded Covariate Shifts. The definition of "semantic" vs. "covariate" shift becomes ambiguous if the learned decision boundary lies in higher levels of the semantic hierarchy. Consider the scenario in Fig. 1 *Middle*, where "dog" and "vehicle" are the only ID classes. The learned classifier can also be considered "animal" vs. "vehicle" classifier. Then, "cat," although technically a semantic shift, can also be considered a *semantically-grounded covariate shift* with the label "animal." This scenario is very similar to subpopulation shift where bias in the data collection

Figure 2: **Examples of Images from ImageNet-OOD.** Images around the 10th, 30th, 50th, 70th, 90th percentile based on either the distance to the closest ImageNet-1K image using features from self-supervised ResNet-50 pre-trained on the PASS dataset (Asano et al., 2021) or scores from OOD detectors MSP (Hendrycks & Gimpel, 2017), Energy (Liu et al., 2020), ViM (Wang et al., 2022), and ReAct (Sun et al., 2021). Within each pair, the left image is the ImageNet-OOD image and the right image is its closest image in ImageNet-1K. These examples illustrate the diversity of ImageNet-OOD and its visual similarity to ImageNet-1K despite having different semantics and OOD scores.

process results in overdomaince of a subclass. Using the WordNet semantic tree, we determine the most general decision boundary for ImageNet-1K. We identify the common ancestor for every pair of ImageNet-1K classes and position each ImageNet-1K class one level below any one of the common ancestors. Subsequently, we redefine all the ImageNet-1K classes to the class defined by this decision boundary during our dataset construction process.

Final Class Selection. Despite removing ambiguous classes, manual effort is still needed to resolve visual ambiguities between ImageNet-1K and the rest of ImageNet-21K images. The authors of ImageNet noted that flaws in the construction process of ImageNet-21K can introduce labeling errors due to visual ambiguity across classes (Russakovsky et al., 2015). For instance, the classes "Viola" and "Violin" are virtually indistinguishable unless compared side by side to discern their sizes, thus bringing some degree of human labeling errors. Consequently, the OOD dataset might be contaminated with images from ID classes. Additionally, certain OOD labels are distant on the WordNet semantic tree but contain images with similar semantics. For instance, nearly all images from "Aqualung" (ImageNet-21K) and "Scuba Diver" (ImageNet-1K) depict a scuba diver wearing an Aqualung, since an Aqualung is an apparatus essential for scuba divers to breathe underwater. To avoid the visual ambiguities illustrated in Fig. 1 *Right*, we spent 20 hours to manually select 637 classes from the remaining set that are distinguishable from ImageNet-1K classes by iteratively examining the WordNet neighbors of each ImageNet-1K class and randomly selecting 50 images. Following this, a final 6-hour review is conducted to filter out any images that might have been mislabeled. This process is described in greater details in Section H of the Appendix.

3.3 IMAGENET-OOD STATISTICS

ImageNet-OOD contains a total of 31,807 images from 637 classes. Our construction methodology naturally results in a dataset that is as diverse as ImageNet-1K and also very similar visually to ImageNet-1K images. To illustrate this, Fig. 2 displays an amalgamation of images that is very diverse in terms of both semantics and visuals, ranging from fried eggs to capacitors, and objects against plain backgrounds to complex scenes. Additionally, the nearest ImageNet-1K image for each ImageNet-OOD image appears to be in a very similar domain.

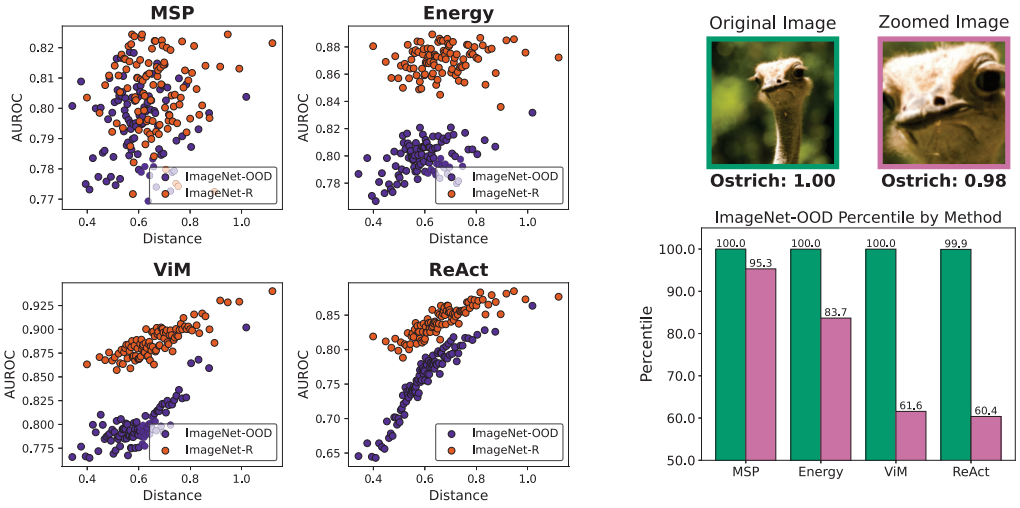

Figure 3: **Influence of Covariate Shift on OOD Detection.** *Left.* Relationship between OOD detection performance and the average distance to the closest ImageNet-1K (Russakovsky et al., 2015) image using features from self-supervised models trained on the PASS (Asano et al., 2021) dataset. Results reveal that given similar PASS feature distances between subsets of the two datasets, modern OOD detection algorithms elicit a stronger response to covariate shift (ImageNet-R (Hendrycks et al., 2020)) than semantic shift (ImageNet-OOD). *Right.* An image of Ostrich in ImageNet-1K dataset where an elementary zoom transformation is applied. The transformation did not influence the model prediction, but substantially decreased the ranking of ViM (Wang et al., 2022) and ReAct (Sun et al., 2021) scores in ImageNet-OOD by 38.4%, 39.6%, respectively.

4 Empirical Analysis

Equipped with ImageNet-OOD, we now analyze the performance of OOD detection algorithms under semantic shift with limited covariate shift. First, we demonstrate that modern OOD detection algorithms are more susceptible to covariate shifts. We reveal that even for images with similar distance to ImageNet-1K, modern OOD detection algorithms perform better at detecting images from covariate shift dataset ImageNet-R (Hendrycks et al., 2020) than images from ImageNet-OOD. Additionally, we design a simple sanity check for OOD detection on random untrained models. Our result show that OOD detection algorithms fails the sanity check and elicit a strong response to covariate shift. Finally, through an extensive evaluation of nine OOD detection algorithms and six datasets over 13 network architectures, we demonstrate that many modern OOD detection algorithms do not draw practical benefits in both new-class detection and failure detection scenarios.

Our experiments include nine logit-based and feature-based OOD detection algorithms, which are more practically adopted due to their require minimal computational cost (Yang et al., 2021b). Logit-based methods MSP (Hendrycks & Gimpel, 2017), Energy (Liu et al., 2020), Max-Cosine (Zhang & Xiang, 2023), and Max-Logit (Hendrycks et al., 2022) derive scoring functions from classification logits because OOD examples tend to have lower activations. Feature-based methods Mahalanobis (Lee et al., 2018), KNN (Sun et al., 2022), ViM (Wang et al., 2022), ASH-B (Djurisic et al., 2022), and ReAct (Sun et al., 2021) operate on the penultimate layer of the model. Hyperparameters are selected based on ablation studies on ImageNet-1K done by original authors.

4.1 Covariate Shifts Confound Detection of Semantic Shift

We begin by demonstrating that modern OOD detectors are highly sensitive to covariate shift. Concretely, they cannot *only* detect a large proportion of semantic shift data without simultaneously detecting a large proportion of covariate shift data. To illustrate this, we partition subsets of images with varying degrees of visual similarity to ImageNet-1K, the ID data, with half the subsets exhibiting covariate shift and half exhibiting semantic shift. Specifically, we partition ImageNet-R (Hendrycks et al., 2020) and ImageNet-OOD datasets into 100 subsets each. In each set, images

have similar distances to the closest ImageNet-1K (Russakovsky et al., 2015) image using features from a MoCo-v2 (Chen et al., 2020) self-supervised ResNet-50 (He et al., 2016) model pre-trained on the PASS dataset (Asano et al., 2021), which is an ImageNet replacement derived from YFCC-100M (Thomee et al., 2016). Next, we feed each image into a ResNet-50 classifier trained on ImageNet-1K to obtain the OOD scores. Finally, we calculate the AUROC between images of each subset and images from ImageNet-1K to analyze the relationship between OOD detection performance (AUROC) and the average PASS distance to the closest ImageNet-1K image of each subset.

We make a number of observations shown in Fig. 3 *Left*. First, as one would expect, there is a positive trend between the OOD detection performance and average PASS distance, as images "farther" from the training distribution have been shown to be easier to detect (Fort et al., 2021). The trend seems to be stronger in modern OOD detection algorithms such as Energy (Liu et al., 2020), ViM (Wang et al., 2022), and ReAct (Sun et al., 2021) than in the baseline MSP (Hendrycks & Gimpel, 2017). More importantly, modern detection algorithms are clearly better at detecting ImageNet-R images than ImageNet-OOD images, even with similar PASS distances. To verify this quantitatively, we fit a linear regression model between PASS distance and AUROC for each of the datasets to account for the effect of PASS distance on AUROC. Our results reveal that for ViM, Energy, and ReAct, the 95% confidence intervals on the intercept of the regression trained between the two datasets do not overlap. As a result, there is statistical significance suggesting that the effect of ImageNet-R naturally induces a higher detection performance than ImageNet-OOD on ViM, Energy, and ReAct. The full results and details are included in the Section C of the appendix.

To further demonstrate that OOD scores are affected by covariate shifts, we illustrate that upon introducing a modest covariate shift, there is a notable decline in the scores of OOD detectors. Fig. 3 *Right* displays an image from ImageNet-1K, depicting an ostrich. A ResNet-50 classifier predicts the image correctly with a confidence score around 100%, which ranks higher than 99% of confidence on ImageNet-OOD images. Three modern OOD detectors also assign a score to this image that ranks it higher than 99% of the images from ImageNet-OOD. After applying a zoom to the ostrich, the classifier still exhibits a high classification confidence score of 98%, which still ranks higher than 95.3% of ImageNet-OOD. However, the OOD detection scores rankings from Energy, ViM, and React drops to only 83.7%, 61.6%, and 61.4% higher than the ImageNet-OOD samples, respectively, despite there being no change in semantic label or model prediction.

4.2 OOD DETECTION ALGORITHMS FAIL SANITY CHECK ON COVARIATE SHIFT DATASETS

After observing how sensitive modern OOD detection algorithms are to covariate shifts, we design a sanity check to further test this sensitivity in a much stronger setting. Previous works demonstrated the power of random models as feature extractors for tasks such as in-painting, super resolution, and interpretability (Adebayo et al., 2018; Saxe et al., 2011; Alain & Bengio, 2016; Ulyanov et al., 2018). While having this power is acceptable for other tasks, it is very problematic in the context of OOD detection as it challenges the fundamental concept of ID and OOD. The idea of ID becomes ill-defined on random models as the model has not encountered or learned from data sampled from any distributions. Therefore, for a randomly initialized model, the concept of ID should not exist.

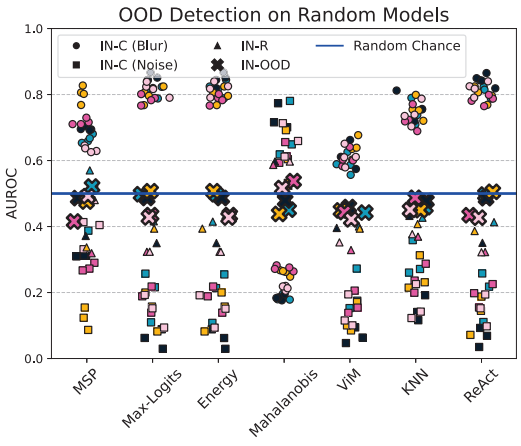

Figure 4: **Performance of OOD detection under random models.** Five ResNet-50 models (indicated by color) with *random* parameters were evaluated on ImageNet-R (IN-R), ImageNet-C (IN-C) and ImageNet-OOD (IN-OOD).

Given that every data point should be considered OOD for a random model, a well-behaved OOD detection algorithm should perform around random chance (AUROC = 0.5) (Hendrycks & Gimpel, 2017). We design a simple sanity check around this idea and found that OOD detection algorithm is biased toward certain covariate shifts. Performance of seven commonly

Table 1: **Performance of OOD Detection Algorithms.** We evaluate seven modern OOD detection algorithms across 13 models, three covariate shift datasets: ImageNet-C (IN-C), ImageNet-R (IN-R), ImageNet-Sketch (IN-Sketch) and two semantic shift datasets: ImageNet-OOD and OpenImage-O, under the goals of both new-class detection and failure detection. Results in each column denotes the AUROC of each pair of **ID** vs. **OOD** datasets. The low AUROCs of the In-C, IN-R, and IN-Sketch vs. IN-OOD experiments indicate that OOD detection algorithms lose their ability to perform new-class detection under the presence of covariate shifts that these datasets introduce. Moreover, the improvement of the best-performing detector is only 0.7% in the IN-1K vs. IN-OOD experiment. The results also confirm that MSP still outperforms all modern methods under failure detection.

Goal	Method	IN-C IN-OOD	IN-R IN-OOD	IN-Sketch IN-OOD	IN-1K OpenImage-O	IN-1K IN-OOD
New-class Detection	MSP	**55.5**	**48.0**	**46.4**	84.6	79.8
	Max-Logit	52.3	40.4	41.0	87.9	80.5
	Energy	51.5	38.9	39.9	87.6	79.9
	Mahalanobis	43.6	37.8	30.7	76.0	64.8
	ViM	46.4	35.9	31.8	88.9	79.8
	KNN	39.7	36.9	26.3	76.0	59.3
	Max-Cosine	55.4	36.3	38.0	85.8	**80.7**
	ASH-B	51.5	46.2	41.8	**90.1**	79.5
	ReAct	41.4	35.0	36.9	82.7	63.4
Failure Detection	MSP	**80.8**	**76.1**	**76.8**	**90.0**	**86.9**
	Max-Logit	76.9	68.9	72.6	89.2	84.1
	Energy	75.5	66.4	70.9	88.5	83.1
	Mahalanobis	57.1	58.4	51.0	74.5	65.9
	ViM	70.7	67.1	64.7	88.7	82.5
	KNN	51.9	52.7	47.2	68.7	55.0
	Max-Cosine	73.5	71.5	72.6	88.5	84.8
	ASH-B	67.7	71.7	70.4	88.3	81.0
	ReAct	60.2	47.9	55.9	80.4	65.7

used OOD detection methods is evaluated using five random models on the ImageNet-R (Hendrycks et al., 2020) images and on blurring and noise corruptions in ImageNet-C (Hendrycks & Dietterich, 2019). This experiment is performed on Resnet-50 with Kaiming normal initialization (He et al., 2015). We use only the most severe corruptions in ImageNet-C.

Fig. 4 reveals that OOD detectors confidently detect blurry ImageNet-C images as OOD (AUROC > 0.5) and noisy ImageNet-C images as ID (AUROC < 0.5). Additionally, they also tend to detect ImageNet-R images as ID. ImageNet-OOD, on the other hand, is unaffected and detected around random chance (AUROC $= 0.5$). The bias toward detecting certain corrupted images illustrates that OOD detectors can easily pick up patterns from covariate shift, even on untrained models.

4.3 Modern OOD detection algorithms do not bring practical benefits

In this section, we show that modern detection algorithms do not gain significant benefits over the MSP (Hendrycks & Gimpel, 2017) baseline regardless of the approach to OOD detection. Under new-class detection, we reveal that when covariate shifts are minimized, modern detection algorithms have less than 1% AUROC improvement over the MSP baseline. Furthermore, comprehensive analysis under failure detection reveals that modern OOD detection algorithms do not actually improve at distinguishing between correctly classified examples and semantically OOD examples.

For the evaluation, we used 13 different convolutional neural networks trained on ImageNet-1K from the torchvision library: ResNet(He et al., 2016), DenseNet (Huang et al., 2017), Wide ResNet (Zagoruyko & Komodakis, 2016), RegNet (Xu et al., 2022), ResNeXt (Xie et al., 2017). The algorithms were evaluated across five different datasets: ImageNet-C (Hendrycks & Dietterich, 2019), ImageNet-R (Hendrycks et al., 2020), ImageNet-Sketch(Wang et al., 2019), OpenImage-O (Wang et al., 2022), and ImageNet-OOD. The results from Table 1 reports the average AUROC across the 13 models under both new-class and failure detection scenarios.

New-class Detection. New-class detection aims to detect only examples from semantic shift datasets. All images that belong to training classes, including covariate shifted examples, are considered ID. We first demonstrate that under the influence of certain covariate shifts, OOD detection algorithms are not able to identify semantic shifts. Table 1 displays AUROC scores on three covariate shift datasets vs. ImageNet-OOD. All detection algorithms show AUROC below 50% on ImageNet-Sketch and ImageNet-R vs. ImageNet-OOD, indicating a less than 50% probability that an OOD detector scores an ImageNet-OOD example higher than an ImageNet-Sketch example. However, MSP yields significantly higher AUROC than other OOD detectors, revealing that modern OOD detectors are more susceptible towards covariate shift.

Next, we demonstrate that improvements gained on past datasets disappear when modern OOD detection algorithms are evaluated on ImageNet-OOD. The discrepancy in AUROC between ImageNet-1K vs. OpenImage-O and ImageNet-1K vs. ImageNet-OOD highlights the importance of the semantic shift dataset. In particular, on OpenImage-O, Max-Logit, ViM, and ASH-B all exhibit significant improvements over the MSP baseline, showing a 3.3%, 4.3%, and 5.5% enhancement in AUROC, respectively. However, when evaluated on ImageNet-OOD, the improvements drastically shrank to 0.7% for Max-Logit, completely disappears for ViM and even decreased by 0.3% for ASH-B. We provide qualitative explanations for this phenomenon in Section G in the Appendix. With the insignificant improvement under semantic shift coupled with the increased susceptibility towards covariate shift, it is unclear whether modern OOD detection algorithms yields any practical improvements over the baseline when deployed to the real-world.

Findings on Failure Detection. Failure detection aims to detect incorrectly classified examples regardless of the type of distribution shift with semantic shift examples being incorrect by definition. Results from Table 1 confirms previous findings that MSP outperforms modern OOD detection algorithms under failure detection across all experiments. Interestingly, on the ImageNet-1K vs. ImageNet-OOD experiment, MSP outperforms Max-Logit by 2.8% under failure detection despite Max-Logit outperforming MSP by 0.7% under new-class detection. This discrepancy is particularly an unexpected outcome since semantic shift examples are considered OOD for both failure and new-class detection. Breaking down the test data by whether or not they are correctly predicted resolves this mystery. Fundamentally, the goal of an OOD detection algorithm is to give lower scores, and hence, lower rankings, on semantic shift data (Equation 1). However, we observe from Fig. 5 that Max-Logit does not rank the semantic shift (ImageNet-OOD) examples lower (more OOD) than MSP does. Instead, it ranks the incorrect test (ImageNet-1K) examples higher. In other words, Max-Logit is neither better at detecting semantic shift examples (Fig. 5 *Right*) nor better at preserving correct test examples (Fig. 5 *Left*). Instead, it is better at preserving incorrect test examples (Fig. 5 *Center*), which is the *opposite* of the ideal behavior for catching model failures.

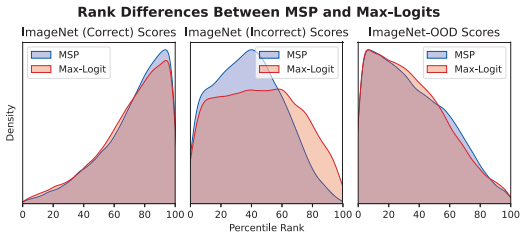

Figure 5: **Comparison of the ranking between MSP and Max-Logit .** *Left.* MSP is slightly better at ranking correctly predicted ImageNet images higher. *Center.* Max-Logit ranks more incorrect ImageNet images higher than MSP. *Right.* MSP and Max-Logits have near identical ranks on ImageNet-OOD examples.

5 Conclusion

We introduce ImageNet-OOD, a carefully curated, diverse OOD detection dataset for studying the effects of semantic shifts. By building on top of ImageNet-21K and manually selecting test classes to remove semantic and visual ambiguities, we avoid unnecessary covariate shifts that may confound the performance of OOD detection algorithms. Using ImageNet-OOD, we reveal that many modern OOD detection algorithms detect covariate shifts to a greater extent than semantic shifts and further demonstrate that the improvement of many algorithms disappears. We hope that our dataset and findings will help the OOD detection community in building methods that are more effective at detecting semantic shifts and aligning their behavior with their stated purpose.

ETHICS STATEMENT

Although our dataset and analysis does not directly produce harmful impact, we note that the bias from ImageNet may be propagated as ImageNet-OOD reuses images from ImageNet-21K (Deng et al., 2009; Yang et al., 2020). As a means of mitigation, we manually filter out inappropriate classes. In addition, OOD detection becomes a high-stake task to prevent catastrophic failures in computer vision systems. While we strive to include a diverse set of classes in ImageNet-OOD, we cannot guarantee that performance on ImageNet-OOD is the a valid indicator for all safety-critical applications.

REPRODUCIBILITY STATEMENT

We provide the class names and synset IDs for all ImageNet-OOD classes in the appendix. In addition, we provide all image filenames as presented in the ILSVRC 2012 Challenge (Russakovsky et al., 2015), as well as sample code for the experiments in the linked Github repository linked in the abstract.

ACKNOWLEDGEMENTS

This material is based upon work supported by the National Science Foundation under Grant No. 2112562. Any opinions, findings, and conclusions or recommendations expressed in this material are those of the authors' and do not necessarily reflect the views of the National Science Foundation. We also thank the Princeton VisualAI Lab members and Christiane Fellbaum for helpful feedback.

REFERENCES

Julius Adebayo, Justin Gilmer, Michael Muelly, Ian Goodfellow, Moritz Hardt, and Been Kim. Sanity checks for saliency maps. *Advances in neural information processing systems*, 31, 2018.

Guillaume Alain and Yoshua Bengio. Understanding intermediate layers using linear classifier probes. *arXiv preprint arXiv:1610.01644*, 2016.

Yuki M Asano, Christian Rupprecht, Andrew Zisserman, and Andrea Vedaldi. Pass: An imagenet replacement for self-supervised pretraining without humans. In *Thirty-fifth Conference on Neural Information Processing Systems Datasets and Benchmarks Track (Round 1)*, 2021.

Reza Averly and Wei-Lun Chao. Unified out-of-distribution detection: A model-specific perspective. In *Proceedings of the IEEE/CVF International Conference on Computer Vision*, pp. 1453–1463, 2023.

Julian Bitterwolf, Maximilian Müller, and Matthias Hein. In or out? fixing imagenet out-of-distribution detection evaluation. In *International Conference on Machine Learning*, pp. 2471–2506. PMLR, 2023.

Xinlei Chen, Haoqi Fan, Ross Girshick, and Kaiming He. Improved baselines with momentum contrastive learning, 2020.

Mircea Cimpoi, Subhransu Maji, Iasonas Kokkinos, Sammy Mohamed, and Andrea Vedaldi. Describing textures in the wild. In *Proceedings of the IEEE conference on computer vision and pattern recognition*, pp. 3606–3613, 2014.

Jia Deng, Wei Dong, Richard Socher, Li-Jia Li, Kai Li, and Li Fei-Fei. Imagenet: A large-scale hierarchical image database. In *2009 IEEE conference on computer vision and pattern recognition*, pp. 248–255. Ieee, 2009.

Li Deng. The mnist database of handwritten digit images for machine learning research. *IEEE Signal Processing Magazine*, 29(6):141–142, 2012.

Andrija Djurisic, Nebojsa Bozanic, Arjun Ashok, and Rosanne Liu. Extremely simple activation shaping for out-of-distribution detection. *arXiv preprint arXiv:2209.09858*, 2022.

Christiane Fellbaum. *WordNet: An Electronic Lexical Database*. Bradford Books, 1998.

Stanislav Fort, Jie Ren, and Balaji Lakshminarayanan. Exploring the limits of out-of-distribution detection. In A. Beygelzimer, Y. Dauphin, P. Liang, and J. Wortman Vaughan (eds.), *Advances in Neural Information Processing Systems*, 2021.

Ido Galil, Mohammed Dabbah, and Ran El-Yaniv. A framework for benchmarking class-out-of-distribution detection and its application to imagenet. In *The Eleventh International Conference on Learning Representations*, 2023.

Joris Guérin, Kevin Delmas, Raul Sena Ferreira, and Jérémie Guiochet. Out-of-distribution detection is not all you need, 2023.

Jiangpeng He and Fengqing Zhu. Out-of-distribution detection in unsupervised continual learning, 2022.

Kaiming He, Xiangyu Zhang, Shaoqing Ren, and Jian Sun. Delving deep into rectifiers: Surpassing human-level performance on imagenet classification. In *Proceedings of the IEEE international conference on computer vision*, pp. 1026–1034, 2015.

Kaiming He, Xiangyu Zhang, Shaoqing Ren, and Jian Sun. Deep residual learning for image recognition. In *2016 IEEE Conference on Computer Vision and Pattern Recognition (CVPR)*, pp. 770–778, 2016. doi: 10.1109/CVPR.2016.90.

Dan Hendrycks and Thomas Dietterich. Benchmarking neural network robustness to common corruptions and perturbations. In *International Conference on Learning Representations*, 2019.

Dan Hendrycks and Kevin Gimpel. A baseline for detecting misclassified and out-of-distribution examples in neural networks. *Proceedings of International Conference on Learning Representations*, 2017.

Dan Hendrycks, Steven Basart, Norman Mu, Saurav Kadavath, Frank Wang, Evan Dorundo, Rahul Desai, Tyler Zhu, Samyak Parajuli, Mike Guo, Dawn Xiaodong Song, Jacob Steinhardt, and Justin Gilmer. The many faces of robustness: A critical analysis of out-of-distribution generalization. *2021 IEEE/CVF International Conference on Computer Vision (ICCV)*, pp. 8320–8329, 2020.

Dan Hendrycks, Kevin Zhao, Steven Basart, Jacob Steinhardt, and Dawn Song. Natural adversarial examples. In *Proceedings of the IEEE/CVF conference on computer vision and pattern recognition*, pp. 15262–15271, 2021.

Dan Hendrycks, Steven Basart, Mantas Mazeika, Andy Zou, Joseph Kwon, Mohammadreza Mostajabi, Jacob Steinhardt, and Dawn Song. Scaling out-of-distribution detection for real-world settings. In *International Conference on Machine Learning*, pp. 8759–8773. PMLR, 2022.

Grant Van Horn, Oisin Mac Aodha, Yang Song, Yin Cui, Chen Sun, Alexander Shepard, Hartwig Adam, Pietro Perona, and Serge J. Belongie. The inaturalist species classification and detection dataset. *2018 IEEE/CVF Conference on Computer Vision and Pattern Recognition*, pp. 8769–8778, 2018.

Yen-Chang Hsu, Yilin Shen, Hongxia Jin, and Zsolt Kira. Generalized odin: Detecting out-of-distribution image without learning from out-of-distribution data. In *Proceedings of the IEEE/CVF conference on computer vision and pattern recognition*, pp. 10951–10960, 2020.

Gao Huang, Zhuang Liu, Laurens Van Der Maaten, and Kilian Q Weinberger. Densely connected convolutional networks. In *Proceedings of the IEEE conference on computer vision and pattern recognition*, pp. 4700–4708, 2017.

Rui Huang and Yixuan Li. Mos: Towards scaling out-of-distribution detection for large semantic space. In *Proceedings of the IEEE/CVF Conference on Computer Vision and Pattern Recognition*, 2021.

Rui Huang, Andrew Geng, and Yixuan Li. On the importance of gradients for detecting distributional shifts in the wild. In *Advances in Neural Information Processing Systems*, 2021.

Paul F Jaeger, Carsten Tim Lüth, Lukas Klein, and Till J. Bungert. A call to reflect on evaluation practices for failure detection in image classification. In *The Eleventh International Conference on Learning Representations*, 2023.

Alex Kendall and Yarin Gal. What uncertainties do we need in bayesian deep learning for computer vision? In I. Guyon, U. Von Luxburg, S. Bengio, H. Wallach, R. Fergus, S. Vishwanathan, and R. Garnett (eds.), *Advances in Neural Information Processing Systems*, volume 30. Curran Associates, Inc., 2017.

Gyuhak Kim, Changnan Xiao, Tatsuya Konishi, Zixuan Ke, and Bing Liu. A theoretical study on solving continual learning. In Alice H. Oh, Alekh Agarwal, Danielle Belgrave, and Kyunghyun Cho (eds.), *Advances in Neural Information Processing Systems*, 2022.

Alex Krizhevsky. Learning multiple layers of features from tiny images. 2009.

Alina Kuznetsova, Hassan Rom, Neil Alldrin, Jasper Uijlings, Ivan Krasin, Jordi Pont-Tuset, Shahab Kamali, Stefan Popov, Matteo Malloci, Alexander Kolesnikov, et al. The open images dataset v4: Unified image classification, object detection, and visual relationship detection at scale. *International journal of computer vision*, 128(7):1956–1981, 2020.

Kimin Lee, Kibok Lee, Honglak Lee, and Jinwoo Shin. A simple unified framework for detecting out-of-distribution samples and adversarial attacks. *Advances in neural information processing systems*, 31, 2018.

Shiyu Liang, Yixuan Li, and R. Srikant. Enhancing the reliability of out-of-distribution image detection in neural networks. In *International Conference on Learning Representations*, 2018.

Weitang Liu, Xiaoyun Wang, John Owens, and Yixuan Li. Energy-based out-of-distribution detection. *Advances in Neural Information Processing Systems*, 2020.

Jose G Moreno-Torres, Troy Raeder, Rocío Alaiz-Rodríguez, Nitesh V Chawla, and Francisco Herrera. A unifying view on dataset shift in classification. *Pattern recognition*, 45(1):521–530, 2012.

Yuval Netzer, Tao Wang, Adam Coates, Alessandro Bissacco, Bo Wu, and Andrew Y. Ng. Reading digits in natural images with unsupervised feature learning. In *NeurIPS Workshop on Deep Learning and Unsupervised Feature Learning 2011*, 2011.

Tal Ridnik, Emanuel Ben-Baruch, Asaf Noy, and Lihi Zelnik-Manor. Imagenet-21k pretraining for the masses. In *Thirty-fifth Conference on Neural Information Processing Systems Datasets and Benchmarks Track (Round 1)*, 2021.

Olga Russakovsky, Jia Deng, Hao Su, Jonathan Krause, Sanjeev Satheesh, Sean Ma, Zhiheng Huang, Andrej Karpathy, Aditya Khosla, Michael Bernstein, Alexander C. Berg, and Li Fei-Fei. ImageNet Large Scale Visual Recognition Challenge. *International Journal of Computer Vision (IJCV)*, 115(3):211–252, 2015. doi: 10.1007/s11263-015-0816-y.

Andrew M Saxe, Pang Wei Koh, Zhenghao Chen, Maneesh Bhand, Bipin Suresh, and Andrew Y Ng. On random weights and unsupervised feature learning. In *International Conference on Machine Learning*, 2011.

Yiyou Sun, Chuan Guo, and Yixuan Li. React: Out-of-distribution detection with rectified activations. In A. Beygelzimer, Y. Dauphin, P. Liang, and J. Wortman Vaughan (eds.), *Advances in Neural Information Processing Systems*, 2021.

Yiyou Sun, Yifei Ming, Xiaojin Zhu, and Yixuan Li. Out-of-distribution detection with deep nearest neighbors. *arXiv preprint arXiv:2204.06507*, 2022.

Bart Thomee, David A. Shamma, Gerald Friedland, Benjamin Elizalde, Karl Ni, Douglas Poland, Damian Borth, and Li-Jia Li. YFCC100m. *Communications of the ACM*, 59(2):64–73, jan 2016. doi: 10.1145/2812802.

Junjiao Tian, Yen-Chang Hsu, Yilin Shen, Hongxia Jin, and Zsolt Kira. Exploring covariate and concept shift for out-of-distribution detection. In *NeurIPS 2021 Workshop on Distribution Shifts: Connecting Methods and Applications*, 2021.

Dmitry Ulyanov, Andrea Vedaldi, and Victor Lempitsky. Deep image prior. In *Proceedings of the IEEE conference on computer vision and pattern recognition*, pp. 9446–9454, 2018.

Sagar Vaze, Kai Han, Andrea Vedaldi, and Andrew Zisserman. Open-set recognition: A good closed-set classifier is all you need. In *International Conference on Learning Representations*, 2022.

Haohan Wang, Songwei Ge, Zachary Lipton, and Eric P Xing. Learning robust global representations by penalizing local predictive power. In H. Wallach, H. Larochelle, A. Beygelzimer, F. d'Alché-Buc, E. Fox, and R. Garnett (eds.), *Advances in Neural Information Processing Systems*, volume 32. Curran Associates, Inc., 2019.

Haoqi Wang, Zhizhong Li, Litong Feng, and Wayne Zhang. Vim: Out-of-distribution with virtual-logit matching. In *Proceedings of the IEEE/CVF Conference on Computer Vision and Pattern Recognition*, 2022.

Xiaolong Wang, Yufei Ye, and Abhinav Gupta. Zero-shot recognition via semantic embeddings and knowledge graphs. In *Proceedings of the IEEE conference on computer vision and pattern recognition*, pp. 6857–6866, 2018.

Guoxuan Xia and Christos-Savvas Bouganis. Augmenting softmax information for selective classification with out-of-distribution data. In *Proceedings of the Asian Conference on Computer Vision*, pp. 1995–2012, 2022.

Jianxiong Xiao, James Hays, Krista A. Ehinger, Aude Oliva, and Antonio Torralba. Sun database: Large-scale scene recognition from abbey to zoo. In *2010 IEEE Computer Society Conference on Computer Vision and Pattern Recognition*, pp. 3485–3492, 2010. doi: 10.1109/CVPR.2010.5539970.

Saining Xie, Ross Girshick, Piotr Dollár, Zhuowen Tu, and Kaiming He. Aggregated residual transformations for deep neural networks. In *Proceedings of the IEEE conference on computer vision and pattern recognition*, pp. 1492–1500, 2017.

Jing Xu, Yu Pan, Xinglin Pan, Steven Hoi, Zhang Yi, and Zenglin Xu. Regnet: Self-regulated network for image classification. *IEEE Transactions on Neural Networks and Learning Systems*, pp. 1–6, 2022. doi: 10.1109/TNNLS.2022.3158966.

Jingkang Yang, Haoqi Wang, Litong Feng, Xiaopeng Yan, Huabin Zheng, Wayne Zhang, and Ziwei Liu. Semantically coherent out-of-distribution detection. In *Proceedings of the IEEE International Conference on Computer Vision*, 2021a.

Jingkang Yang, Kaiyang Zhou, Yixuan Li, and Ziwei Liu. Generalized out-of-distribution detection: A survey. *arXiv preprint arXiv:2110.11334*, 2021b.

Jingkang Yang, Kaiyang Zhou, and Ziwei Liu. Full-spectrum out-of-distribution detection. *International Journal of Computer Vision*, 131(10):2607–2622, 2023.

Kaiyu Yang, Klint Qinami, Li Fei-Fei, Jia Deng, and Olga Russakovsky. Towards fairer datasets: Filtering and balancing the distribution of the people subtree in the imagenet hierarchy. In *Proceedings of the 2020 conference on fairness, accountability, and transparency*, pp. 547–558, 2020.

Sergey Zagoruyko and Nikos Komodakis. Wide residual networks. In Edwin R. Hancock Richard C. Wilson and William A. P. Smith (eds.), *Proceedings of the British Machine Vision Conference (BMVC)*, pp. 87.1–87.12. BMVA Press, September 2016. ISBN 1-901725-59-6. doi: 10.5244/C.30.87.

Jingyang Zhang, Jingkang Yang, Pengyun Wang, Haoqi Wang, Yueqian Lin, Haoran Zhang, Yiyou Sun, Xuefeng Du, Kaiyang Zhou, Wayne Zhang, et al. Openood v1. 5: Enhanced benchmark for out-of-distribution detection. *arXiv preprint arXiv:2306.09301*, 2023.

Zihan Zhang and Xiang Xiang. Decoupling maxlogit for out-of-distribution detection. In *Proceedings of the IEEE/CVF Conference on Computer Vision and Pattern Recognition*, pp. 3388–3397, 2023.

Yao Zhu, Yuefeng Chen, Xiaodan Li, Rong Zhang, Hui Xue, Xiang Tian, Rongxin Jiang, Bolun Zheng, and Yaowu Chen. Rethinking out-of-distribution detection from a human-centric perspective, 2022.

APPENDIX

In this appendix, we will provide more detailed analysis on claims made in the main paper.

- **Section A**: We provide an related work on covariate shifts in OOD detection, failure detection, and different OOD detection datasets used in the paper.
- **Section B**: We extend Section 4.1 of the main paper to analyze the difference between score distributions across multiple OOD detection algorithms.
- **Section C**: We supplement Section 4.1 of the main paper on quantitative results using PASS (Asano et al., 2021) distances.
- **Section D**: We analyze the behavior of methods developed for Open-Set Recognition and gradient-based OOD detection.
- **Section E**: We supplement Section 4.3 of the main paper and provide more analysis on the separability between correct and incorrect ID examples.
- **Section F**: We supplement Section 4.2 of the main paper and perform the sanity check to examine covariate shift bias from different model architectures.
- **Section G**: We supplement Section 4.3 of the main paper to provide qualitative examples of images revealing the inherent bias of modern detectors towards certain covariate shift.
- **Section H**: We supplement Section 3 of the main paper and provide details on the construction process of the ImageNet-OOD dataset.
- **Section I**: We supplement Section 3 of the main paper and provide class names and synset IDs for the 637 ImageNet-OOD classes.

A RELATED WORK

Covariate shift in OOD detection. Covariate shift was first considered in OOD detection by Generalized ODIN (Hsu et al., 2020), where OOD detection performance was evaluated considering all covariate shifted examples as out-of-distribution. (Tian et al., 2021) designed a scoring function that disentangles detection of semantic vs. covariate shifts. Later, (Yang et al., 2023) pointed out that models should ideally generalize, instead of detect, in the case of covariate shifts, because generalization is the primary goal of machine learning. Thus, they defined all covariate shifted examples as in-distribution and proposed several benchmarks that include covariate shifted data. Recently proposed benchmark OpenOODv1.5 (Zhang et al., 2023) coined the term full-spectrum detection to encapsulate this idea. They found that under this setting, OOD detection performance are significantly hindered in contrast to the traditional setting. While new-class detection characterizes all covariate shifted examples as ID, failure detection only characterize the correctly classified ones as ID, since the rejection of covariate shift examples that would otherwise hurt the model's classification performance should not be penalized.

Failure Detection. OOD detection is often categorized as a sub-task of failure detection, as the primary goal of OOD detection is to catch unsafe prediction before models make a mistake. Other tasks that share this common goal of failure detection include misclassification detection (Hendrycks & Gimpel, 2017) and uncertainty calibration (Kendall & Gal, 2017), both of which differs from OOD detection in that they do not consider examples outside the set of training classes. However, since all failure detection methods can be interpreted as scoring functions and are motivated from a common principle (alerting failure before occurrence), (Jaeger et al., 2023) argues that all failure detection tasks should be evaluated across a common benchmark that takes into account the classification performance of the model. (Xia & Bouganis, 2022) made similar arguments under Selective Classification in the presence of OOD Data (SCOD).

Datasets for OOD detection. In the experiments of the paper, we used three covariate shift datasets: ImageNet-R (Hendrycks et al., 2020), ImageNet-C (Hendrycks & Dietterich, 2019), and ImageNet-Sketch (Wang et al., 2019). ImageNet-R has 30,000 images containing renditions of 200 ImageNet-1K classes. These renditions include art, cartoons, deviantart, graffiti, embroidery, graphics, origami, paintings, patterns, plastic objects, plush objects, sculptures, sketches, tattoos,

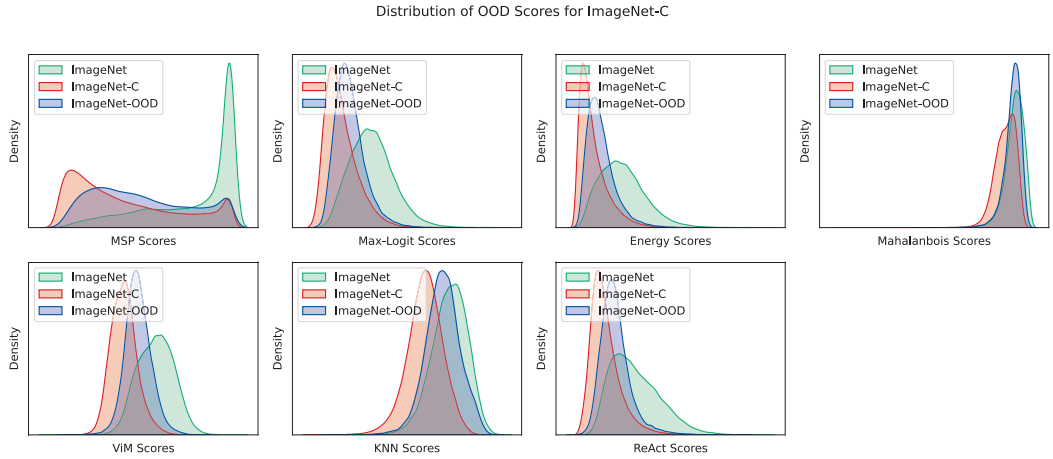

Figure 6: **Distribution of OOD scores on ImageNet-C.** A kernel density estimator further illustrates that all OOD detectors detect covariate shift. Results reveal that for both covariate shift datasets ImageNet-C, the distribution of scores is lower than that of semantic shift.

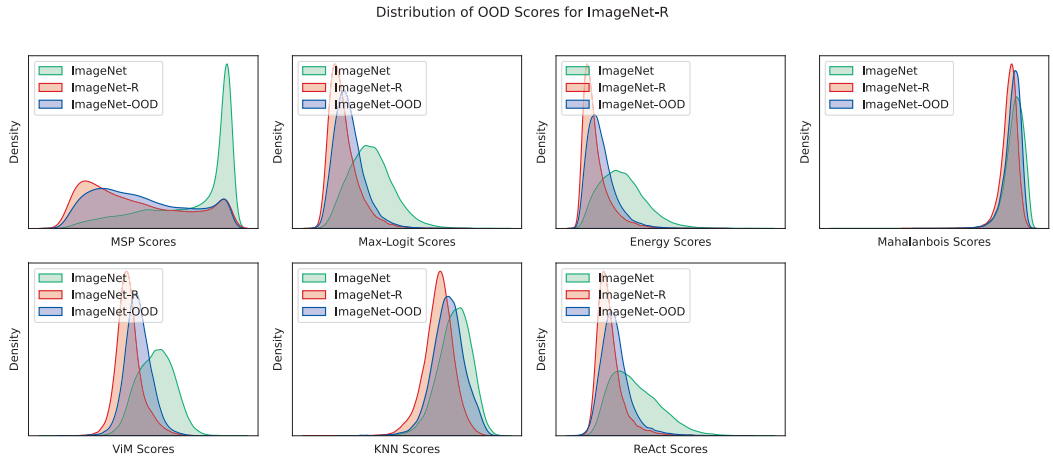

Figure 7: **Distribution of OOD scores on ImageNet-R.** Same setup as Figure 6 but on ImageNet-R and reaches the same conclusion.

toys, and video games. ImageNet-C includes corrupted versions of ImageNet-1K images at different severity levels using corruptions such as brightness, contrast, elastic, pixelate, and JPEG. ImageNet-Sketch contains 50,000 images of sketches of all ImageNet-1K classes. We also used OpenImage-O (Wang et al., 2022), a manually curated semantic shift dataset, which is derived from OpenImages (Kuznetsova et al., 2020), an object detection dataset.

B Analysis of score distributions

In the following experiment, we will compare the score distributions of OOD detectors on semantic and covariate shift datasets to further show that that OOD detectors cannot *only* reject a large proportion of semantic shift data without simultaneously rejecting a large proportion correctly classified covariate shift data.

We provide complete analysis across seven OOD detection algorithms on their distribution of scores between covariate and semantic shift. Fig. 6 and 7 shows that all seven algorithms rank a significant proportion of covariate shift examples lower than semantic shift examples. Additionally, breaking down covariate shift examples between correct vs. incorrect, Fig. 8 and 9 reveals that all seven

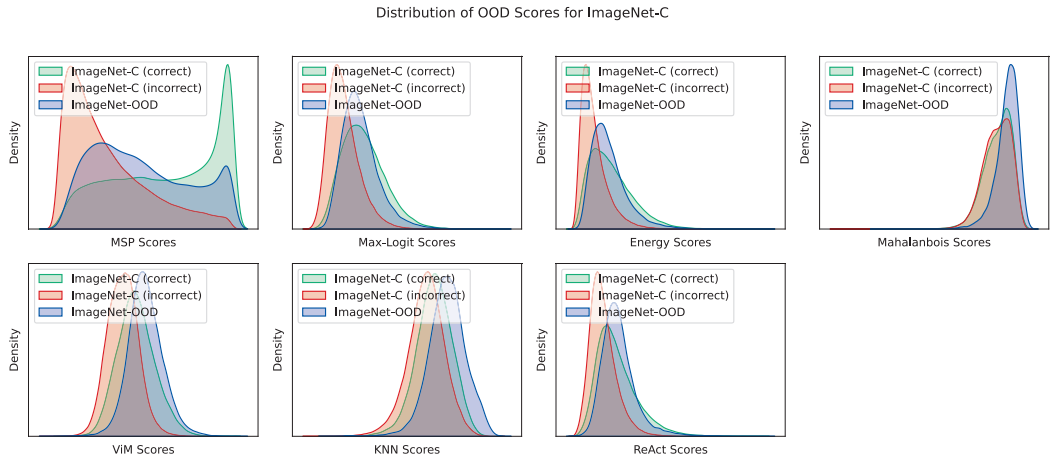

Figure 8: **Score breakdown on covariate shift data on ImageNet-C.** Comparison of detection score distributions for correctly classified covariate shift examples on ImageNet-C and semantic shift examples (ImageNet-OOD). Scores of correct ImageNet-C examples tend to be even lower than ImageNet-OOD examples. Rejecting a significant portion of semantic shift data leads to the rejection of a significant portion of correct covariate shift data.

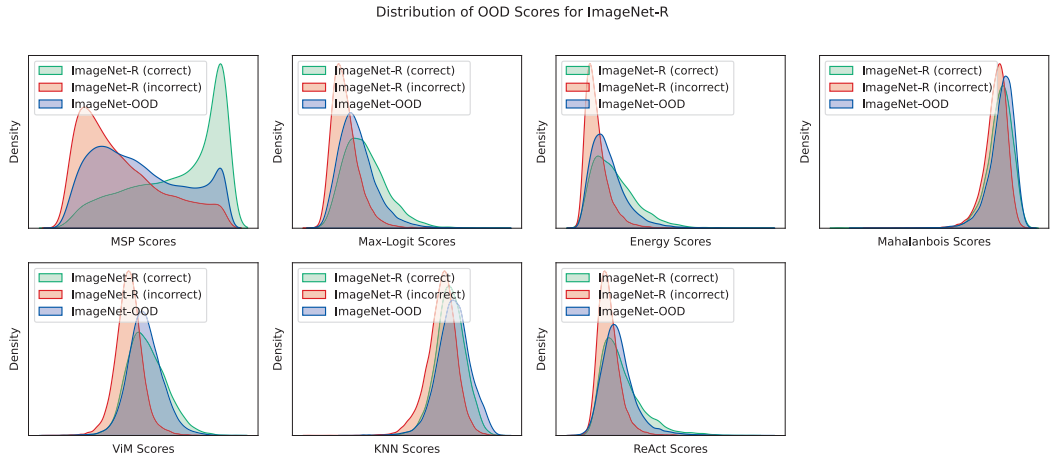

Figure 9: **Score breakdown on covariate shift data on ImageNet-R.** Same setup as Figure 8 but on ImageNet-R. Scores of correct ImageNet-C examples tend to be similar to ImageNet-OOD examples.

Table 2: **Proportion of correct examples discarded by rejecting 75 percent of ImageNet-OOD examples.** Using the threshold where 75 percent of ImageNet-OOD examples are rejected as OOD, how many correct examples from ImageNet-1K, ImageNet-C, and ImageNet-R are discarded, which hurt model safety. Results reveals that modern OOD detection methods does not show significant lower false rejection rate on ImageNet-1K and have significantly worse false rejection rate when covariate shift is introduced by ImageNet-C and ImageNet-R.

	ImageNet (Russakovsky et al., 2015)	ImageNet-C (Hendrycks & Dietterich, 2019)	ImageNet-R (Hendrycks et al., 2020)
MSP (Hendrycks & Gimpel, 2017)	18	**53.6**	**41.9**
Max-Logit (Hendrycks et al., 2022)	**17.8**	65.6	58.7
Energy (Liu et al., 2020)	19.3	67.4	61.2
Mahalanobis (Lee et al., 2018)	59.0	91.7	80.2
ViM (Wang et al., 2022)	22.2	85.3	68.8
KNN (Sun et al., 2022)	57.8	92.3	83.1
ReAct (Sun et al., 2021)	27.1	73.5	68.0

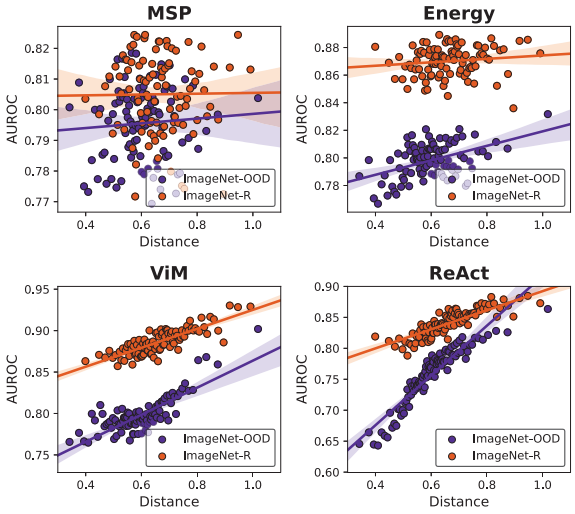

Method	Dataset		Value	SE
MSP	IN-R	β	0.001	0.011
		α	0.804	0.007
	IN-OOD	β	0.008	0.011
		α	0.791	0.007
Energy	IN-R	β	0.012	0.009
		α	0.862	0.006
	IN-OOD	β	0.052	0.010
		α	0.767	0.006
ViM	IN-R	β	0.114	0.007
		α	0.812	0.005
	IN-OOD	β	0.163	0.121
		α	0.701	0.007
ReAct	IN-R	β	0.154	0010
		α	0.738	0.007
	IN-OOD	β	0.515	0.010
		α	0.402	0.016

Figure 10: **Full Analysis on influence of Covariate Shift on OOD Detection.** *Left.* Relationship between OOD detection performance and the average distance to the closest ImageNet-1K (Russakovsky et al., 2015) image using features from self-supervised pre-trained models on the PASS (Asano et al., 2021) dataset. This figure adds a linear regression model with its 95% confidence interval to Fig. 3. The results augments findings in section 4.1 by revealing substantial overlap in confident region in MSP but low overlap for Energy, ViM, and ReAct. *Right.* Quantitative measures for each of the fitted linear model with given form AUROC $= \beta(\text{distance}) + \alpha$. The 95% confidence interval for the α between the two datasets do not overlap for Energy, ViM, and ReAct, but do overlap for MSP. This means that the difference in intercept coefficient is statistically significant for Energy, ViM, and ReAct but not MSP.

algorithms do indeed confuse correctly classified covariate shift examples with semantic shift examples. Finally, Table 2 uncovers that all seven algorithms yield significantly more rejection of correctly classified examples with covariate shift datasets. This provide comprehensive support for the conclusion drawn in Section 3.2 of the main paper.

C Quantitative analysis on PASS distances

In this section, we provide full details on the quantitative measures of the relationship between PASS (Asano et al., 2021) distance (image similarity) and AUROC (OOD detection performance). The results in Fig. 10 *Right* confirms that there is a statistical significant difference on the performance of OOD detection between covariate shift (ImageNet-R) and semantic shift (ImageNet-OOD). Using the standard error, we can derive the 95% confidence interval for the intercept measure of the linear regression model. For example, using two times the standard error, we can derive for energy the respective confidence interval between ImageNet-R and ImageNet-OOD as (0.85, 0.874) and (0.755, 779). Since these two intervals do not overlap, there is statistical significance that the real intercept between the two datasets is different. Intuitively, the intercept of the model measure the effect of dataset independent from PASS distance on OOD detection performance. Since it appears the intercept for the ImageNet-R model is higher, this suggests covariate shifts tend to boost AUROC, demonstrating that OOD detectors detect covariate shift more easily. Similar conclusions can be reached for ViM and ReAct, but not MSP, revealing modern algorithms are more susceptible to covariate shifts. Fig. 10 *Left* unravel the performance different between the two datasets across different PASS measures. We observe that the confident region of the linear regression model have substantial overlaps for MSP and minor overlap for ReAct. On other hand, Energy and ViM have no overlap within the specified interval, indicating that the modern detectors are more affected by covariate shift than MSP.

Table 3: **OOD detection performance for ResNet-50 under Gradient-based OOD and OpenMax.** OOD detection performance for Open-Set Recognition and gradient-based OOD detection methods on the two semantic shift datasets suggest the same conclusion: MSP baseline is best for failure detection and modern methods do not have substantial improvement over baseline once spurious covariate shift is removed. ODIN$_\epsilon$ uses $T = 1000$ and $\epsilon = 0.0014$. ODIN uses $T = 1000$ with no adversarial perturbations. GradNorm uses $T = 1$.

Goal	Method	OpenImage-O	ImageNet-OOD
New-class Detection	MSP	84.0	79.2
	ODIN$_\epsilon$	86.5	80.1
	ODIN	87.4	**80.4**
	GradNorm	80.4	73.8
	OpenMax	**87.4**	80.2
Failure Detection	MSP	**89.9**	**86.8**
	ODIN$_\epsilon$	87.9	83.5
	ODIN	89.3	84.6
	GradNorm	77.2	72.2
	OpenMax	88.5	83.4

Table 4: **Detailed breakdown of AUROC performance with respect to ImageNet-OOD.** Breakdown reveals that the improvement observed in both Max-Logit and Energy is attributed to better separation between incorrect ID predictions and OOD predictions, shown by the large margin of increase in AUROC between Incorrect ID (+) vs. OOD (-). Performance between correct in-distribution predictions and out-of-distribution predictions are similar. Additionally, when evaluating incorrect ID predictions vs. correct ID predictions, separability decreases for Max-Logit and Energy compared to MSP.

	Correct ID (+) vs. OOD (-)	Incorrect ID (+) vs. OOD (-)	Correct ID (+) vs. Incorrect ID (-)
MSP (Hendrycks & Gimpel, 2017)	86.9	54.7	86.4
Max-Logit (Hendrycks et al., 2022)	86.3	61.8	77.7
Energy (Liu et al., 2020)	85.4	62.4	76.2

D Open-Set recognition and gradient-based OOD detection

Open-Set Recognition (OSR) is a similar task to semantic OOD detection, where the goal is to identify unseen classes. Gradient-based OOD detection algorithms uses some aspects on the gradients of a model to calculate an OOD score. Since detection requires the calculation of gradient on each image, such method of OOD detection is more computationally expensive. We perform the same analysis from 4.3 but on a single ResNet-50 model on the popular OSR algorithm OpenMax (Hsu et al., 2020) which does not require any retraining and gradient-based OOD detection algorithm ODIN (Liang et al., 2018) and GradNorm (Huang et al., 2021) on OpenImage-O and ImageNet-OOD. Results from Table 1 reveals the same consistent behavior where we see substantial improvement from MSP on OpenImage-O but not ImageNet-OOD for new-class detection, and the MSP baseline outperforms these methods for failure detection.

E Additional experiments for detection of incorrect examples

In addition to the analysis that visualizes the ranking of OOD scores in Section 4.3, we quantitatively examine AUROC on ImageNet-OOD to measure the separability between three groups of examples: correctly classified in-distribution (ID) examples, incorrectly classified ID examples, and semantic shifted OOD examples.

Specifically, since AUROC is a measure of separability (*i.e.* the probability of scoring a positive example higher than a negative example), we examine the AUROC among these three groups of examples. Using the probabilistic interpretation of AUROC, we can decompose AUROC between

ID vs. OOD by correct ID and incorrect ID using the law of total probability:

$$\begin{aligned} &p(f(x_{in}) > f(x_{out})) = \\ &p(f(x_{in}) > f(x_{out})|C(x_{in}) = 1)p(C(x_{in}) = 1) + \\ &p(f(x_{in}) > f(x_{out})|C(x_{in}) = 0)p(C(x_{in}) = 0) \end{aligned} \tag{2}$$

where x_{in}, x_{out} refer to semantic ID and OOD examples, respectively, f is the OOD scoring function, and C is an indicator function with $C(x) = 1$ if x is predicted correctly, and 0 otherwise.

Table 4 reports $p(f(x_{in}) > f(x_{out})|C(x_{in}) = 1)$ (*i.e.* column Correct ID (+) vs. OOD (-)) and $p(f(x_{in}) > f(x_{out})|C(x_{in}) = 0)$ (*i.e.* column Incorrect ID (+) vs. OOD (-)). The results reveal increased separability between incorrect ID vs. OOD from MSP to ViM and ReAct, decreased separability between correctly classified ID vs. incorrectly classified ID, and roughly the same separability between correctly classified vs. OOD. Since $p(C(x_{in}) = 1)$ in Equation 2 is the classification accuracy on the ID dataset, we see that for 71.6% of increase in new-class detection AUROC from ViM can be attributed to an increase in performance of detecting Incorrect ID vs. OOD predictions. This pattern supports the claim that many advanced OOD detection methods improve under the old benchmark by detecting more incorrectly classified examples as ID rather than a balanced improvement across the ID set.

Additionally, we also use AUROC to approximate the probability of scoring correct ID higher than incorrect ID examples, reported in the Correct ID (+) vs. Incorrect ID (-) column in Table 4. We found that advanced OOD detection methods have lower separability between correctly classified ID vs. incorrectly classified ID. Having lower separability between correct vs. incorrect hurts the performance of the model from a safety perspective, as more problematic examples can pass through the OOD detection filter.

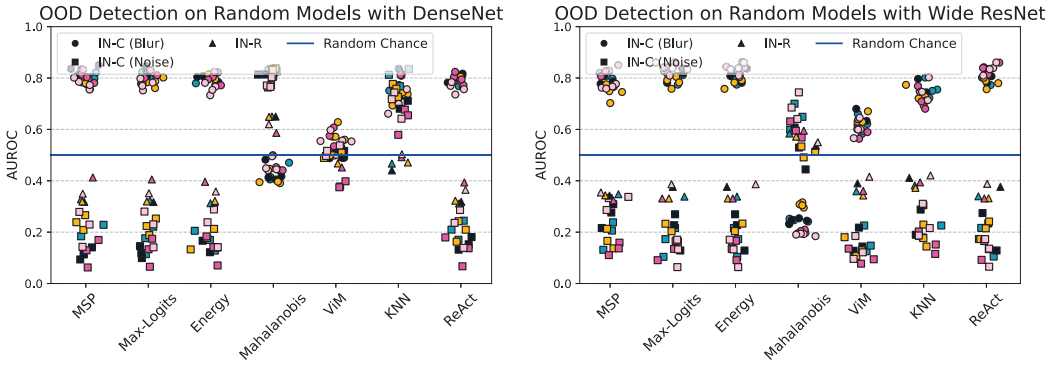

Figure 11: **OOD detection performance under random models.** AUROC performance of 5 DenseNet-121 models (*left*) or 5 Wide ResNet-50 model (*right*) with **random**, untrained parameters on subsets of ImageNet-C (Hendrycks & Dietterich, 2019) under the existing benchmark vs our proposed benchmark. Colors indicate the specific random model and the markers indicate the corruption type. Results reveals the same conclusion as the ResNet-50 sanity check.

F Sanity check extends to other model architectures

We expand our analysis of the sanity check in Section 4.2 to other model architectures and to the scenario of failure detection. For architectures, we display additional random DenseNet-121 (Huang et al., 2017) and Wide ResNet-50 (Zagoruyko & Komodakis, 2016). Results from Figure 11 reveal that the same issue with sanity check occurs on DenseNet, except ViM, and Wide Resnet-50 in the scenario of new-class detection, suggesting that this issue applies to convolution based architecture.

G Qualitative Analysis on Covariate Shift Bias

We expand our analysis by visualizing images where modern OOD detection algorithms and the baseline MSP differ the most. We perform this analysis on ImageNet-1K, ImageNet-OOD, OpenImage-O, and ImageNet-Sketch on a ResNet-50 model trained on ImageNet-1K. We found that modern OOD detection algorithms ViM and ASH-B tends to latch on to specific spurious features that are exacerbated by dataset with uncontrolled covariate shift, confounding their evaluation on semantic shift.

We reveal in Figure 12 that the OOD detection method ViM tends to give texture-like images low scores, detecting them as OOD. This effect is more prominent in OpenImage-O because it appears there are many images in a different domain. In contrast, our dataset ImageNet-OOD has images more similar to ImageNet-1K. The observed change in domain is a clear example of unnecessary covariate shifts, explaining the vanishing performance gains of ViM in ImageNet-OOD. Similarly in Figure 13, we observe that the OOD detection algorithm ASH-B tends to score text-like images as OOD. Though there are some imperfections due to the class semantics (e.g. map is an object but also can be a diagram), ImageNet-OOD overall still produced more similar looking images to ImageNet-1K.

In summary, qualitative analysis on the discrepancy between modern OOD detection algorithms and MSP motivate our dataset: the minimization of covariate shift is important when assessing an OOD detector's performance on semantic shift for the task of new-class detection.

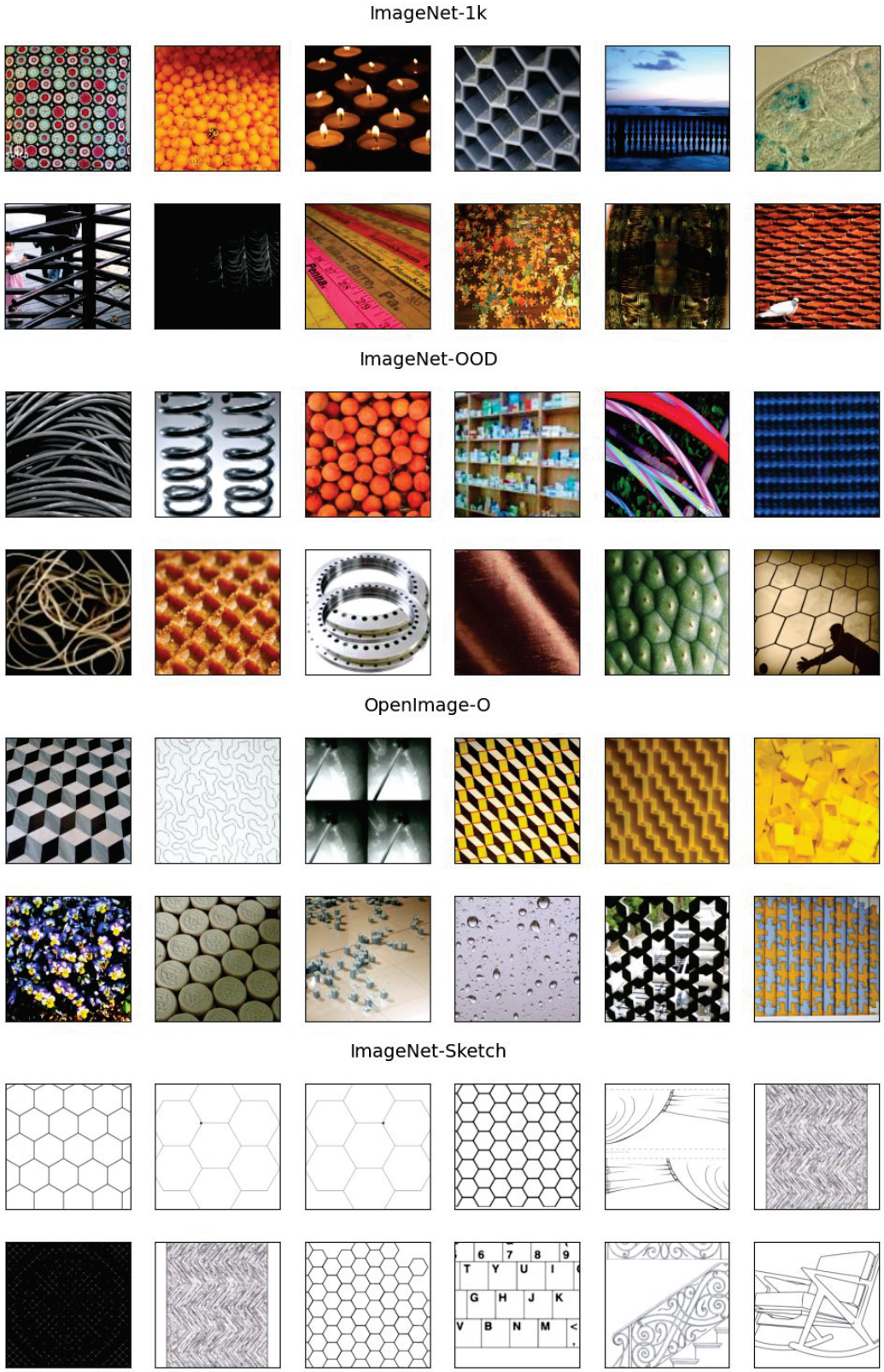

Figure 12: **Images with highest discrepancy in ranks between ViM and MSP.** We show 12 images from ImageNet-1K, ImageNet-OOD, OpenImage-O, and ImageNet-Sketch with the highest discrepancy in ranks where ViM scores low (OOD) and MSP scores high (ID) revealing that ViM tends to prefer detecting texture as OOD. The images also reveal that ImageNet-OOD images are more realistic and comparable to ImageNet-1K than OpenImage-O.

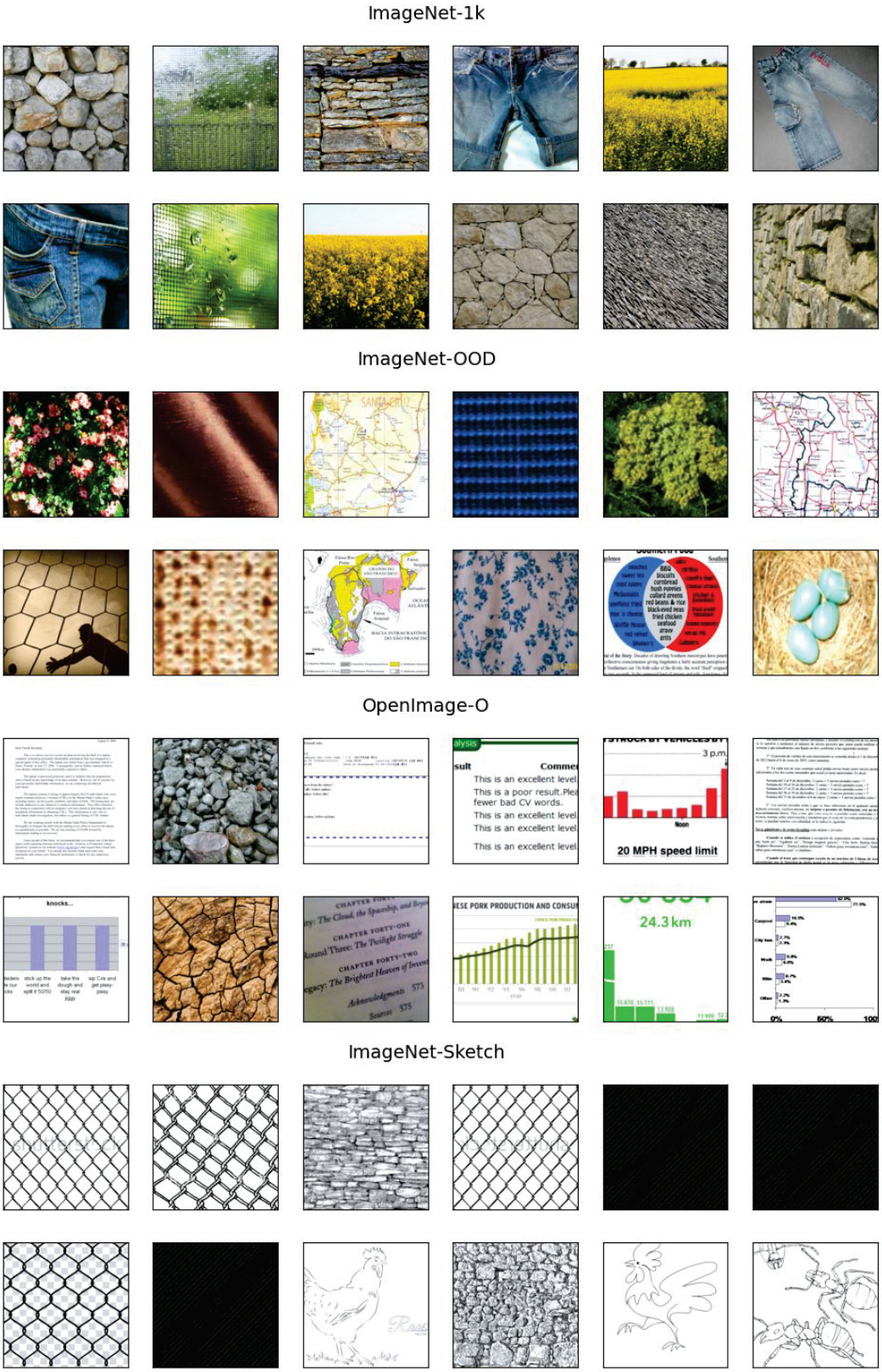

Figure 13: **Images with highest discrepancy in ranks between ASH-B and MSP.** We show 12 images from ImageNet-1K, ImageNet-OOD, OpenImage-O, and ImageNet-Sketch with the highest discrepancy in ranks where ASH-B scores low (OOD) and MSP scores high (ID) revealing that ASH-B tends to prefer detecting text as OOD.

H MORE DETAILS ON IMAGENET-OOD CONSTRUCTION

In this section, we provide details on the manual selection process of ImageNet-OOD. Because images from ID classes may leak into OOD classes if human labelers are unable to disambiguate two classes, such as "violin" and "viola" (Russakovsky et al., 2015), we manually selected 1000 classes from ImageNet-21K to construct ImageNet-OOD. However, even after excluding hypernyms, hyponyms, and the "organism" subtree, there are still 5074 remaining candidate ImageNet-21K classes. It is simply infeasible to check all 5074 classes against all 1000 ImageNet-1K classes, which would require $5074 \times 1000 = 5,074,000$ manual comparisons. Therefore, we need to employ another mechanism that can pass through the 5074 classes in linear time.

To start the collection process, we aim to pick out 1000 classes, We first gathered the sister classes for each ImageNet-1K class. A sister class c_s^i is defined as a class that shares a direct parent with an ImageNet-1K class c^i. For example, the sister classes for the ImageNet-1K class "microwave" has sister classes "food_processor", 'ice_maker", "hot_plate", "coffee_maker", and "oven", because these classes all have the same direct parent "kitchen_appliance." Considering only sister classes allowed us to further reduce the search space down to 2874 candidate classes.

Once we had obtained the sister classes, we examined the visual and semantic ambiguity between each sister class and its corresponding ImageNet-1K class through example images. Unambiguous classes are added to the final list of ImageNet-OOD classes. Since the ambiguity between classes was considered during the curation of ImageNet-1K classes, we assume that there exists minimal ambiguity between classes under different subtrees that contains an ImageNet-1K class. This assumption allowed us to only examine the relationship of sister classes with their corresponding ImageNet-1K class instead of with all 1000 ImageNet-1K classes. In the end, we only needed to compare 13,831 pairs of classes.

Following the manual selection of the 1000 classes, we filtered out the classes with semantically-grounded covariate shift using the method described in Section 3. Then, we examined the 1000 images that are the closest to ImageNet-1K validation images in terms of ResNet-50 (He et al., 2016) feature distance to filter out visual similarity. We filter out both classes and images. Classes such as "aqualung" (visually similar to ID class "scuba diver") were filtered out in this stage, and images with indistinguishable visuals were also thrown out. The final resulting dataset will include 31,807 images from 637 classes.

I IMAGENET-OOD CLASSES

Synset ID	Class Name	Synset ID	Class Name
n02666943	abattoir	n04108822	rope_bridge
n02678897	adapter	n04113406	roulette_wheel
n02688273	air_filter	n04114844	router
n02689434	air_hammer	n04116098	rubber_band
n02698634	alpenstock	n04118635	ruin
n02705429	amphora	n04119230	rumble_seat
n02705944	amplifier	n04122685	sachet
n02710044	andiron	n04123740	saddle
n02723165	antiperspirant	n04132603	samisen
n02725872	anvil	n04134008	sandbag
n02726681	apartment_building	n04136800	sash_fastener
n02757337	audiometer	n04139140	saucepot
n02758960	autoclave	n04150153	scouring_pad
n02763604	aviary	n04150980	scraper
n02767956	backbench	n04167346	seeder
n02768226	backboard	n04168199	Segway
n02770721	backscratcher	n04171831	semiconductor_device
n02770830	backseat	n04176068	serving_cart
n02775897	Bailey_bridge	n04176190	serving_dish
n02776205	bait	n04182152	shadow_box

Continued on next page

Synset ID	Class Name	Synset ID	Class Name
n02783994	baluster	n04184435	shaper
n02786331	bandbox	n04186051	shaving_cream
n02799323	baseball_cap	n04190376	shelf_bracket
n02806379	bat	n04198722	shiv
n02807523	bath_oil	n04200258	shoebox
n02807616	bathrobe	n04200537	shoehorn
n02808185	bath_salts	n04206356	shotgun
n02811618	battle_cruiser	n04210120	shredder
n02812949	bayonet	n04211219	shunter
n02816656	beanbag	n04218564	silencer
n02817031	bearing	n04219424	silk
n02821202	bedpan	n04221823	simulator
n02823586	beer_garden	n04224842	sitar
n02826068	bell_jar	n04228215	ski_binding
n02831237	beret	n04228693	ski_cap
n02841187	binnacle	n04233124	skyscraper
n02843553	bird_feeder	n04237423	slicer
n02851939	blindfold	n04238321	slide_fastener
n02855089	blower	n04248851	snare
n02868975	bone-ash_cup	n04252331	snowshoe
n02869249	bones	n04252653	snow_thrower
n02874442	bootjack	n04253057	snuffbox
n02877266	bottle	n04258333	solar_heater
n02879087	bouquet	n04258859	soldering_iron
n02880842	Bowie_knife	n04260364	sonogram
n02881757	bowler_hat	n04269270	spark_plug
n02882190	bowling_alley	n04270891	spear
n02882301	bowling_ball	n04272389	spectator_pump
n02882647	bowling_pin	n04273285	speculum
n02887489	brace	n04282494	splint
n02890940	brake_shoe	n04284869	sport_kite
n02892948	brass_knucks	n04287747	spray_gun
n02893608	breadbasket	n04289027	sprinkler
n02893941	bread_knife	n04290259	spur
n02895438	breathalyzer	n04292921	squeegee
n02903204	broadcaster	n04303357	staple_gun
n02904803	brocade	n04303497	stapler
n02905036	broiler	n04306592	stator
n02910145	bucket_seat	n04314914	step
n02911332	buffer	n04315342	step-down_transformer
n02925009	bushel_basket	n04320973	stirrup
n02927764	butter_dish	n04326896	stool
n02928608	button	n04331639	straightener
n02939866	caliper	n04335886	streetlight
n02940385	call_center	n04344003	stud_finder
n02944579	camouflage	n04346157	stun_gun
n02947660	canal_boat	n04358117	supercomputer
n02951703	canopic_jar	n04364160	surge_suppressor
n02952237	canopy	n04364545	surgical_instrument
n02955247	capacitor	n04373894	sword
n02956699	capitol	n04386051	tailstock
n02957008	capote	n04387095	tam
n02960690	carabiner	n04389854	tank_engine
n02960903	carafe	n04392113	tape
n02962061	carboy	n04409128	tender
n02962200	carburetor	n04414675	Tesla_coil
n02967782	carpet_sweeper	n04417180	textile_machine

Continued on next page

Synset ID	Class Name	Synset ID	Class Name
n02970685	car_seat	n04419073	theodolite
n02973017	cartridge_holder	n04421872	thermometer
n02973904	carving_knife	n04432662	ticking
n02976249	case_knife	n04438897	tin
n02977330	cashmere	n04442441	toaster_oven
n02978055	casket	n04449966	tomahawk
n02981024	catacomb	n04450749	tongs
n02982232	catapult	n04451318	tongue_depressor
n02986160	cattle_guard	n04452528	tool_bag
n02988066	C-clamp	n04453156	toothbrush
n02993194	cenotaph	n04453390	toothpick
n02993368	censer	n04469514	trampoline
n02998003	cereal_box	n04474035	transporter
n03005033	chancellery	n04477387	treadmill
n03005285	chandelier	n04479939	trestle_bridge
n03011355	checker	n04482177	tricorn
n03014440	chessman	n04483073	trigger
n03019685	chin_rest	n04483925	trimmer
n03027250	chuck	n04488202	trophy_case
n03029445	churn	n04489817	trowel
n03030353	cigar_box	n04495698	tudung
n03033362	circuit	n04495843	tugboat
n03034405	circuitry	n04496872	tumbler
n03041114	cleat	n04497801	tuning_fork
n03049924	cloth_cap	n04502502	tweed
n03050655	clothes_dryer	n04502851	twenty-two
n03051249	clothespin	n04520784	vane
n03061674	cockpit	n04525821	Venn_diagram
n03063199	coffee_filter	n04526964	ventilator
n03064758	coffin	n04532831	vibraphone
n03066359	coil_spring	n04533199	vibrator
n03067093	cold_cathode	n04538552	vise
n03075097	comb	n04540255	volleyball_net
n03080633	compass	n04554406	washboard
n03082807	compressor	n04556408	watch_cap
n03087069	concrete_mixer	n04559166	water_cooler
n03089753	conference_center	n04568069	weathervane
n03097362	control_center	n04568841	webbing
n03099147	convector	n04579056	whiskey_bottle
n03101664	cookie_jar	n04582869	wicket
n03103563	coonskin_cap	n04586581	winder
n03105088	copyholder	n04589325	window_box
n03105467	corbel	n04590746	windshield_wiper
n03115400	cotton_flannel	n04594489	wire
n03119510	coupling	n04606574	wrench
n03122073	covered_bridge	n04613939	Zamboni
n03133415	crock	n04615226	zither
n03140431	cruet	n06275095	cable
n03141702	crusher	n07579688	piece_de_resistance
n03150232	curler	n07579917	adobo
n03156767	cylinder_lock	n07580359	casserole
n03158885	dagger	n07591961	paella
n03161450	damper	n07593471	viand
n03175457	densitometer	n07594066	cake_mix
n03176386	denture	n07607138	chocolate_kiss
n03176594	deodorant	n07611991	mousse
n03180504	destroyer	n07613815	jello

Continued on next page

Synset ID	Class Name	Synset ID	Class Name
n03219135	doll	n07617708	plum_pudding
n03229244	dowel	n07617932	corn_pudding
n03232543	drain_basket	n07618119	duff
n03233744	drawbridge	n07618432	chocolate_pudding
n03235327	drawknife	n07621618	garnish
n03235796	drawstring_bag	n07624466	turnover
n03240892	drill_press	n07641928	fish_cake
n03247083	dropper	n07642361	fish_stick
n03249342	drugstore	n07648913	buffalo_wing
n03250279	drumhead	n07648997	barbecued_wing
n03253796	duffel	n07654148	barbecue
n03254046	duffel_coat	n07654298	biryani
n03254862	dulcimer	n07655263	saute
n03255899	dumpcart	n07665438	veal_parmesan
n03256166	dump_truck	n07666176	veal_cordon_bleu
n03261776	earphone	n07680313	bap
n03266371	eggbeater	n07680517	breadstick
n03267468	ejection_seat	n07680761	brown_bread
n03272125	electric_hammer	n07681450	challah
n03282295	embassy	n07681691	cinnamon_bread
n03287351	energizer	n07682197	crouton
n03293741	equalizer	n07682316	dark_bread
n03296081	escapement	n07682477	English_muffin
n03309356	eyepatch	n07682624	flatbread
n03326795	felt	n07682808	garlic_bread
n03329663	ferry	n07684164	matzo
n03331077	fez	n07684517	raisin_bread
n03342127	finger-painting	n07685730	rye_bread
n03345837	fire_extinguisher	n07686720	sour_bread
n03350204	fishbowl	n07686873	toast
n03351434	fishing_gear	n07687053	wafer
n03356982	flannel	n07696527	butty
n03359566	flask	n07696625	ham_sandwich
n03363749	flintlock	n07696728	chicken_sandwich
n03364599	float	n07696839	club_sandwich
n03367410	florist	n07696977	open-face_sandwich
n03367545	floss	n07697699	Sloppy_Joe
n03378174	food_processor	n07697825	bomber
n03379828	footbridge	n07698250	gyro
n03392741	franking_machine	n07698401	bacon-lettuce-tomato_sandwich
n03397266	frigate	n07698543	Reuben
n03397947	Frisbee	n07698672	western
n03398228	frock_coat	n07698782	wrap
n03407369	fuse	n07708124	julienne
n03420801	garrison_cap	n07709172	potherb
n03423479	gas_heater	n07713267	pieplant
n03423719	gasket	n07713763	mustard
n03429288	gauge	n07715221	brussels_sprouts
n03430418	gazebo	n07723039	leek
n03431745	gearing	n07730406	celery
n03432129	gearshift	n07733394	gumbo
n03440682	glockenspiel	n07750736	Jordan_almond
n03442756	goal	n07750872	apricot
n03448590	gorget	n07753743	passion_fruit
n03451711	graduated_cylinder	n07755411	melon
n03456024	gravy_boat	n07758680	grape
n03456665	greatcoat	n07762114	papaw

Continued on next page

Synset ID	Class Name	Synset ID	Class Name
n03460040	grinder	n07762740	ackee
n03466493	guided_missile_cruiser	n07765073	date
n03469903	gunnysack	n07765999	jujube
n03475823	hairdressing	n07770763	pumpkin_seed
n03490119	hand_truck	n07775197	sunflower_seed
n03490884	hanger	n07806221	salad
n03494537	harmonium	n07817871	fennel
n03495039	harness	n07823951	curry
n03497352	hasp	n07830593	hot_sauce
n03505133	headrest	n07832416	pesto
n03505504	headscarf	n07835457	hollandaise
n03506184	headstock	n07835921	bourguignon
n03506727	hearing_aid	n07837362	white_sauce
n03507241	hearth	n07838073	gravy
n03542333	hotel	n07840027	veloute
n03542605	hotel-casino	n07841495	boiled_egg
n03548402	hula-hoop	n07842202	poached_egg
n03549473	hunting_knife	n07842308	scrambled_eggs
n03553019	hydrofoil	n07842433	deviled_egg
n03565288	imprint	n07842605	shirred_egg
n03571625	ink_bottle	n07842753	omelet
n03572107	inkle	n07843464	souffle
n03572321	inkwell	n07843636	fried_egg
n03589513	jack	n07849336	yogurt
n03609397	kazoo	n07861557	coq_au_vin
n03610682	kepi	n07861813	chicken_and_rice
n03612965	kettle	n07862244	bacon_and_eggs
n03614782	keyhole	n07862348	barbecued_spareribs
n03615790	khukuri	n07862461	beef_Bourguignonne
n03625355	knit	n07862611	beef_Wellington
n03626760	knocker	n07864756	chicken_Kiev
n03628215	koto	n07864934	chili
n03631177	lace	n07865196	chop_suey
n03641569	lanyard	n07865484	chow_mein
n03645011	latch	n07866015	croquette
n03659809	lever	n07866151	cottage_pie
n03659950	lever_lock	n07866277	rissole
n03668067	lightning_rod	n07866409	dolmas
n03680858	lobster_pot	n07866723	egg_roll
n03699591	machete	n07866868	eggs_Benedict
n03718212	man-of-war	n07867021	enchilada
n03719743	mantilla	n07867164	falafel
n03720163	map	n07867324	fish_and_chips
n03721047	marble	n07867421	fondue
n03725600	Mason_jar	n07868200	French_toast
n03742019	medicine_ball	n07868340	fried_rice
n03743279	megaphone	n07868508	frittata
n03760944	microtome	n07868830	galantine
n03765561	mill	n07868955	gefilte_fish
n03767112	millstone	n07869522	corned_beef_hash
n03774327	miter_box	n07869611	jambalaya
n03775388	mixer	n07869775	kabob
n03784270	monstrance	n07870313	seafood_Newburg
n03789946	motor	n07871436	meatball
n03795269	mouthpiece	n07872593	moussaka
n03797182	muffler	n07873464	pilaf
n03802007	musket	n07874780	porridge

Continued on next page

Synset ID	Class Name	Synset ID	Class Name
n03805280	nailfile	n07875436	risotto
n03814817	neckerchief	n07876651	Scotch_egg
n03819448	nest_egg	n07877299	Spanish_rice
n03820318	net	n07877675	steak_tartare
n03836451	nut_and_bolt	n07877849	pepper_steak
n03839671	observatory	n07878647	stuffed_peppers
n03840823	octant	n07878926	stuffed_tomato
n03844045	oil_lamp	n07879072	succotash
n03858418	ottoman	n07879174	sukiyaki
n03865557	overpass	n07879350	sashimi
n03875955	paintball_gun	n07879450	sushi
n03883524	pannier	n07879659	tamale
n03884926	pantheon	n07879953	tempura
n03887185	paper_fastener	n07880213	terrine
n03890093	parer	n07880325	Welsh_rarebit
n03890514	pari-mutuel_machine	n07880458	schnitzel
n03897943	patch	n07880751	taco
n03901229	pavior	n07881404	tostada
n03904909	peeler	n07929351	coffee_bean
n03919430	pestle	n07933154	tea_bag
n03920641	pet_shop	n07937461	couscous
n03923379	phial	n07938149	vitamin_pill
n03923918	phonograph_needle	n09451237	supernova
n03936466	pile_driver	n09818022	astronaut
n03937931	pillion	n09834699	ballet_dancer
n03938037	pillory	n09846755	beekeeper
n03938401	pillow_block	n09913593	cheerleader
n03939178	pilot_boat	n10091651	fireman
n03941231	pinata	n10366966	nurse
n03941417	pinball_machine	n10514429	referee
n03941684	pincer	n10521662	reporter
n03946076	pipe_cutter	n10772092	weatherman
n03948950	piston	n11706761	avocado
n03952576	pizzeria	n11851578	prickly_pear
n03955489	plane_seat	n11877283	kohlrabi
n03967396	plotter	n11879054	bok_choy
n03968293	plug	n12088223	yam
n03968581	plughole	n12136392	rattan
n03973628	pocketknife	n12158031	gourd
n03977592	police_boat	n12158443	pumpkin
n03983612	poplin	n12172364	okra
n03993180	pouch	n12246232	blueberry
n03996416	power_shovel	n12301445	olive
n04000311	press	n12333771	guava
n04011827	propeller	n12352990	plantain
n04013729	prosthesis	n12373100	papaya
n04015908	protractor	n12399132	mulberry
n04016846	psaltery	n12400489	breadfruit
n04020298	pulley	n12433081	onion
n04022332	pump	n12441183	asparagus
n04024862	punnet	n12501202	tamarind
n04039848	radar	n12515925	chickpea
n04041243	radiator_cap	n12544539	lentil
n04043411	radio-phonograph	n12560282	pea
n04049753	rain_stick	n12578916	cowpea
n04050933	ramekin	n12636224	medlar
n04051549	ramp	n12638218	plum

Continued on next page

Synset ID	Class Name	Synset ID	Class Name
n04054670	rasp	n12642090	wild_cherry
n04063154	record_changer	n12648045	peach
n04064401	record_player	n12709103	pomelo
n04071263	regalia	n12709688	grapefruit
n04072960	relay	n12711984	lime
n04075291	remote_terminal	n12713063	kumquat
n04075916	repair_shop	n12744387	litchi
n04079933	resistor	n12761284	mango
n04082562	retainer	n12771192	persimmon
n04093625	rink	n12805146	currant
n04093775	riot_gun	n12911673	tomatillo
n04095577	riveting_machine	n13136316	bean
n04097760	roaster	n13136556	nut
n04098513	rocker		